Recent selected results from RHIC Beam Energy Scan Program (and ALICE)

Bedanga Mohanty
NISER

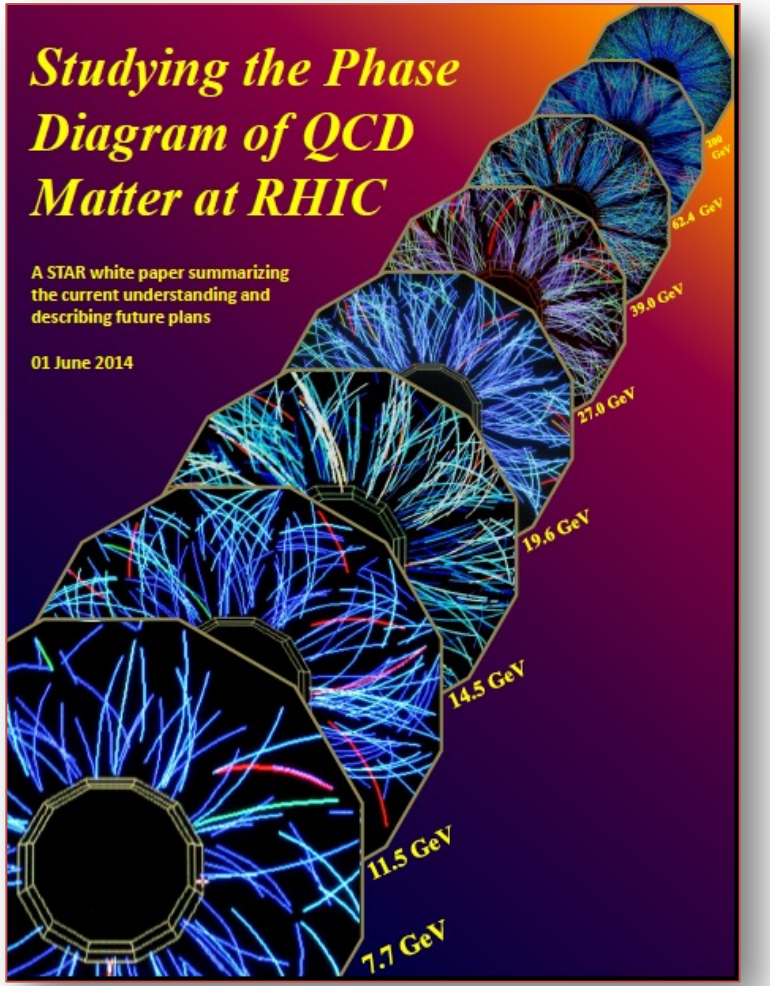

RHIC Beam Energy Scan Program (1)

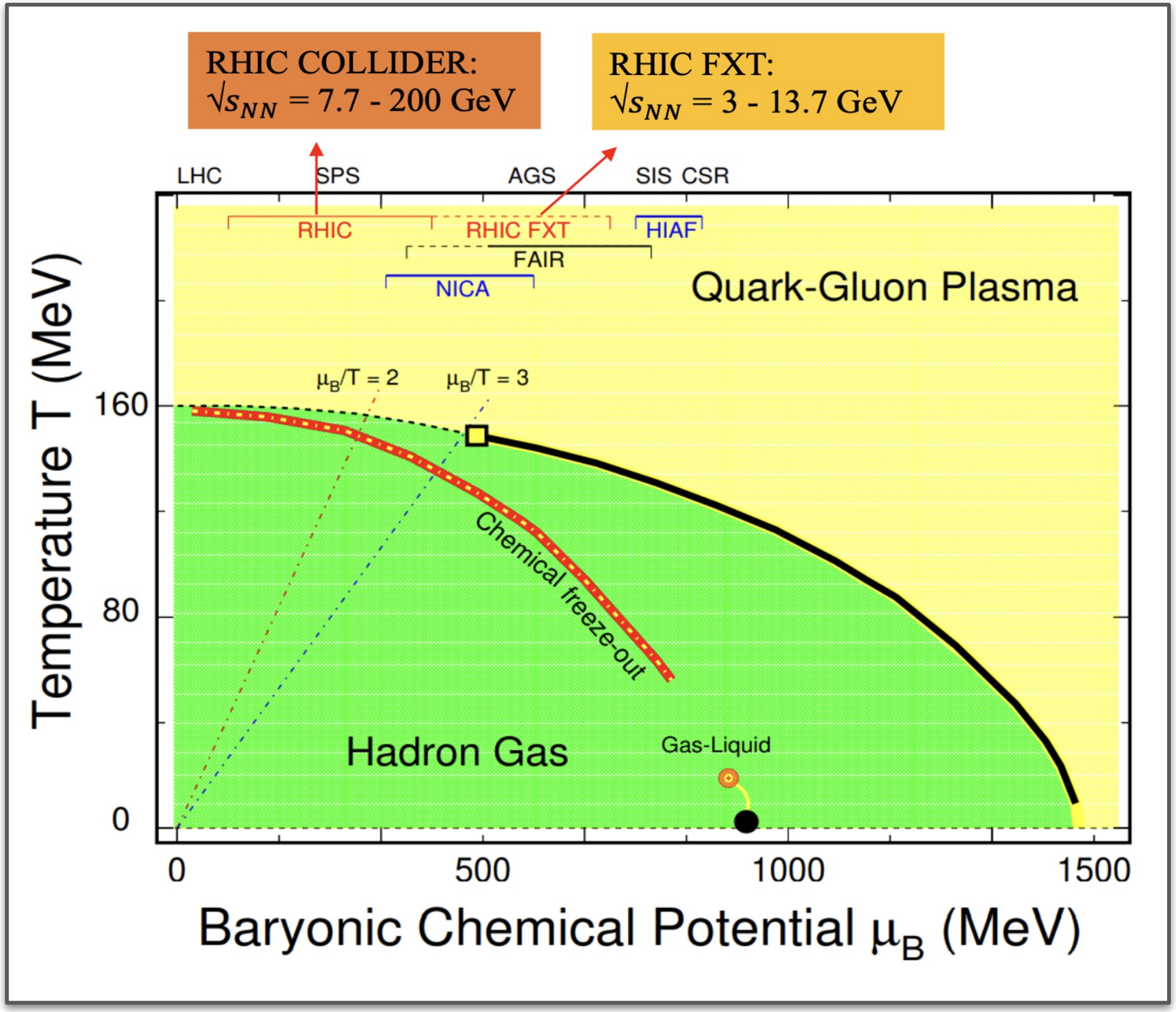

Prog.Part.Nucl.Phys. 125 (2022) 103960

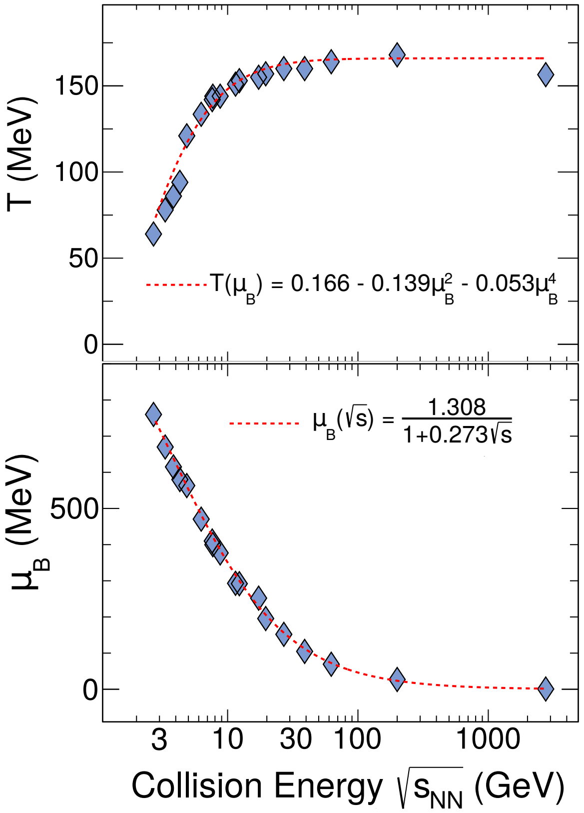

RHIC

RHIC BES Program:

1. First-order phase transition
2. QCD critical end point
3. Turn-off of QGP signatures

RHIC Beam Energy Scan Program (2)

ETOF (-1.6 < η < -1.1,
-2.1 < η < -1.5 in FXT)

iTPC (-1.5 < η < 1.5)

FST, sTGC (2.5 < η < 4.0)

FCS, ECAL (2.5 < η < 4.0)

FCS, HCAL
(2.5 < η < 4.0)

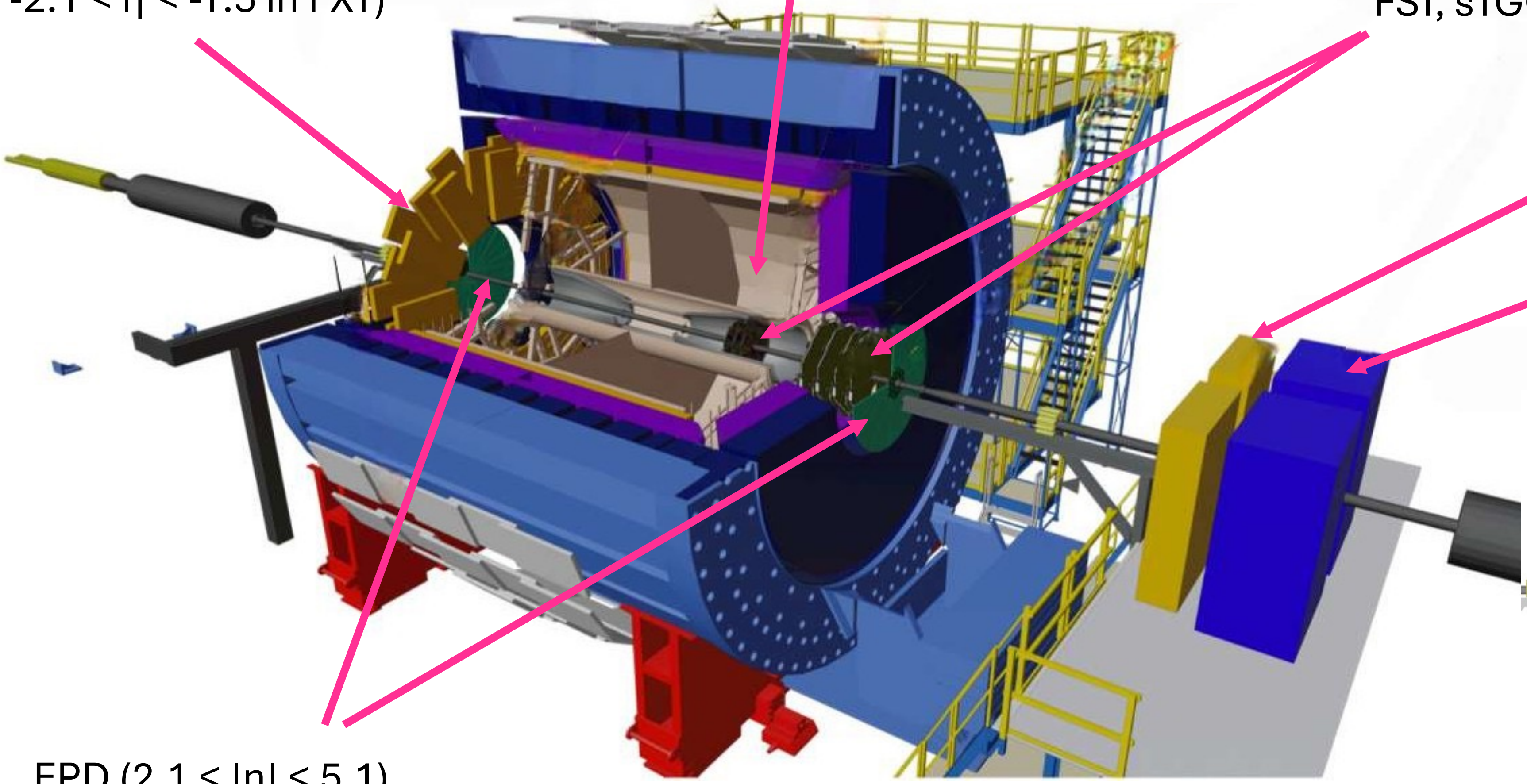

EPD (2.1 < |η| < 5.1)

STAR as fixed collider

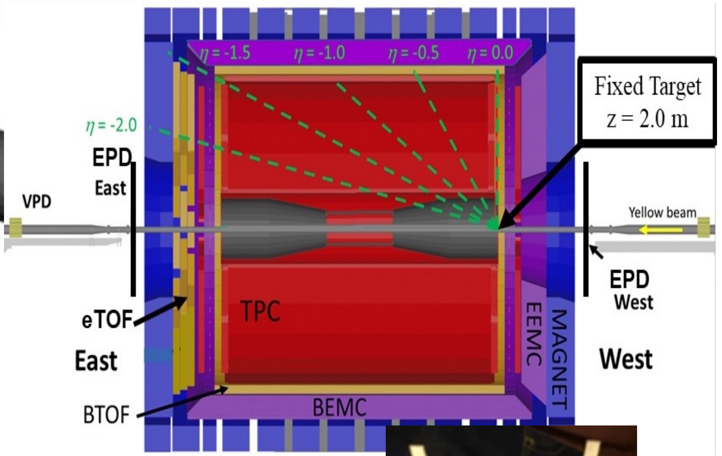

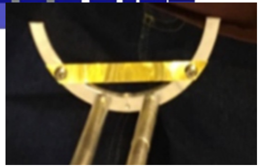

STAR as fixed target

Target is 0.25 mm thick (1% interaction probability) and held 2 cm below center of beam axis

RHIC Beam Energy Scan Program (3)

Au+Au Collisions at RHIC											
Collider Runs						Fixed-Target Runs					
	$\sqrt{s_{NN}}$ (GeV)	#Events	μ_B	y_{beam}	run		$\sqrt{s_{NN}}$ (GeV)	#Events	μ_B	y_{beam}	run
1	**200**	2000 M	**25** MeV	5.3	Run-14, 16	1	13.7 (100)	50 M	280 MeV	-2.69	Run-21
2	62.4	46 M	75 MeV		Run-10	2	11.5 (70)	50 M	320 MeV	-2.51	Run-21
3	54.4	1200 M	85 MeV		Run-17	3	9.2 (44.5)	50 M	370 MeV	-2.28	Run-21
4	39	86 M	112 MeV		Run-10	4	7.7 (31.2)	260 M	420 MeV	-2.1	Run-18, 19, 20
5	27	585 M	156 MeV	3.36	Run-11, 18	5	7.2 (26.5)	470 M	440 MeV	-2.02	Run-18, 20
6	19.6	595 M	206 MeV	3.1	Run-11, 19	6	6.2 (19.5)	120 M	490 MeV	1.87	Run-20
7	17.3	256 M	230 MeV		Run-21	7	5.2 (13.5)	100 M	540 MeV	-1.68	Run-20
8	14.6	340 M	262 MeV		Run-14, 19	8	4.5 (9.8)	110 M	590 MeV	-1.52	Run-20
9	11.5	235 M	316 MeV		Run-10, 20	9	3.9 (7.3)	120 M	633 MeV	-1.37	Run-20
10	9.2	160 M	372 MeV		Run-10, 20	10	3.5 (5.75)	120 M	670 MeV	-1.2	Run-20
11	7.7	104 M	420 MeV		Run-21	11	3.2 (4.59)	200 M	699 MeV	-1.13	Run-19
						12	**3.0** (3.85)	2000 M	**760** MeV		Run-18, 20

25

760

Phase-I : $\sqrt{s_{NN}}$ = 7.7, 11.5, 14.5, 19.6, 27, 39, 62.4, and 200 GeV **(COL)**

Phase-II $\sqrt{s_{NN}}$ = 7.7, 9.2, 11.5, 14.6, 19.6, 27 and 54. 4 GeV **(COL);**
$\sqrt{s_{NN}}$ = 3.0, 3.2, 3.5, 3.9, 4.5, 5.2, 6.2, 7.7, 9.1, 11.5, and 13.7 GeV **(FXT)**

Synergy: RHIC-BES and NICA (1)

Prog.Part.Nucl.Phys. 125 (2022) 103960

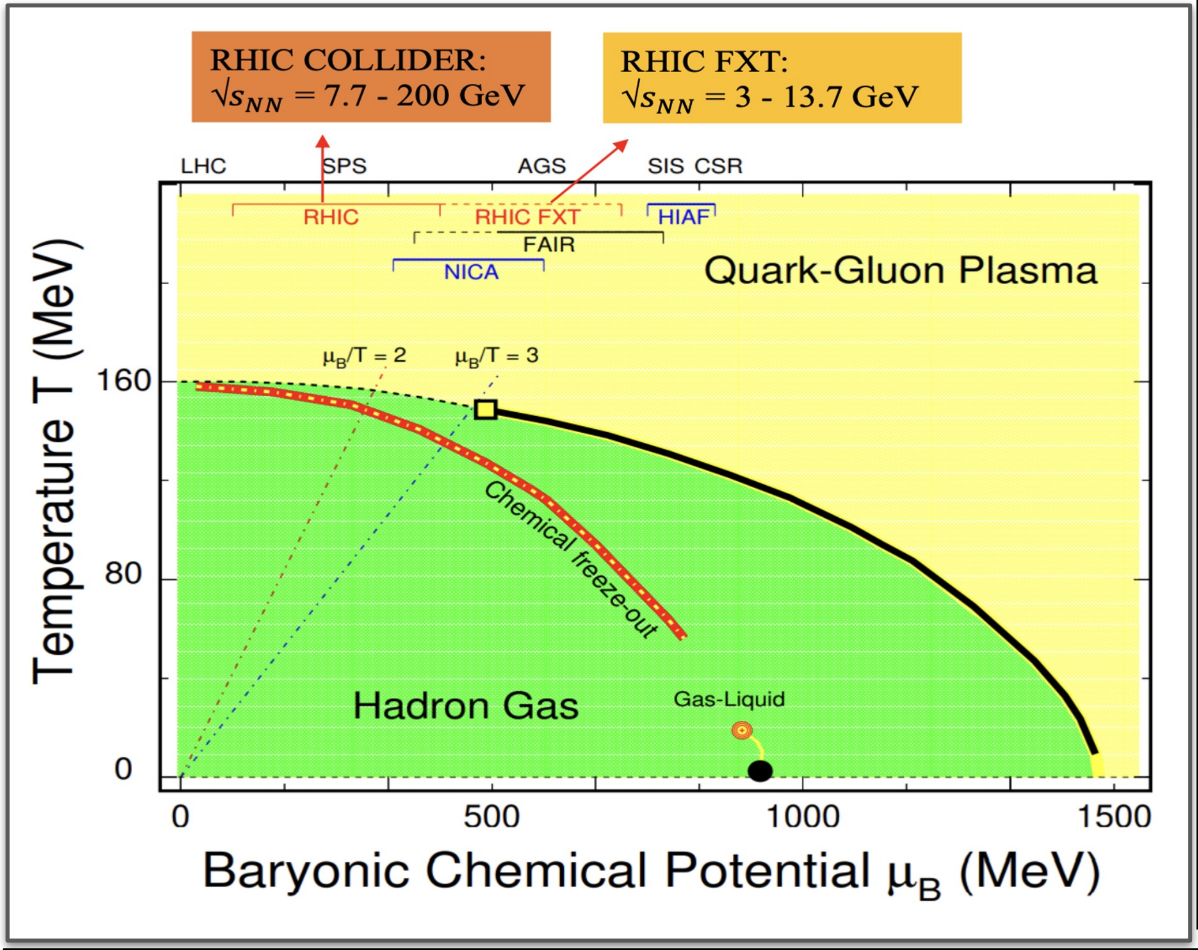

Facility	$\sqrt{s_{nn}}$ (GeV)	μ_B (MeV)	Temperature (MeV) Hadronic / QGP	Key focus
RHIC BES (Phase-II)	3 – 200	25 – 750	100 – 160 > 300	Search for QCD critical point, onset of deconfinement, Vorticity/Polarisation/Spin alignment
NICA (MPD collider)	4 – 11	300 – 700	100 – 160 > 300	EOS, CP, phase coexistence, dense baryonic matter, Vorticity/Polarisation/Spin alignment

RHIC BES + NICA together form a coherent, complementary program to explore the QCD phase diagram across a continuous range of temperature and baryon density.

Synergy: RHIC-BES and NICA (2)

Physics topic	RHIC BES contribution	NICA complementarity
QCD Critical Point	Looking for non-monotonic fluctuations of net-protons, kaons, net-charge	Extend to higher μ_B, better statistics at lower energies
Chiral symmetry restoration	Vector meson spectral shapes, dileptons	Lower energies → denser baryon environment for chiral studies
Collective flow & EOS	v_1, v_2, v_3, directed flow of identified hadrons	Study of EoS at higher baryon densities; softest-point search
Baryon stopping & transport	Net-baryon rapidity distribution	High μ_B sensitivity, test transport models
Strangeness enhancement & hypernuclei	Light hypernuclei and anti-hypernuclei yields	Higher baryon density regime enhances hypermatter production
Spin polarization & vorticity	**Global Λ polarization**, axial effects	Denser medium: test vorticity and chiral effects under high μ_B

Synergy: RHIC-BES and NICA (3)

Detector Component	STAR (RHIC-BES)	MPD (NICA-JINR)	Synergy / Common Strength
Overall Design	Solenoidal 0.5 T magnet; large acceptance	Solenoidal magnet; large acceptance	Similar geometry → transferable tracking & flow methodologies
Primary Tracker	**TPC** + **iTPC upgrade** (extended η, improved dE/dx)	**TPC** with modern electronics	Almost identical central tracker → shared algorithms for tracking, distortions, dE/dx
Tracking Reconstruction	Kalman filtering; cluster finding; space-charge corrections learned from BES-II	Similar Kalman-based tracker & distortion-correction framework	STAR's BES-II calibration recipes directly applicable to MPD
PID: Time-of-Flight	MRPC-based TOF barrel (~80 ps)	MRPC-based TOF barrel (~70–80 ps)	Same PID technology → common calibration, slewing/T0 correction methods
PID: dE/dx	High-precision TPC dE/dx	TPC-based dE/dx	Nearly identical dE/dx PID schemes for π/K/p/e
Centrality / Event Plane	EPD (scintillator tiles) + TPC/TOF multiplicity	FHCal + forward scintillators	Similar event-plane and centrality strategies (spectator-based)
Strange-Hadron Reconstruction	V0, cascade, and hypernuclei via TPC+TOF	Same methods: V0 finder, cascading topologies	High transferability of reconstruction code and topological cuts
Light Nuclei / Hypernuclei	d, t, He-3, hypertriton via TPC+TOF	Same approach planned	STAR templates guide MPD optimization at low √s
Resonance Reconst.	Invariant-mass with TPC+TOF	Same approach	Directly compatible analysis workflows
Flow Analyses	TPC + EPD; cumulants up to 6th order	TPC + forward detectors	Identical detector concept enables comparable flow/cumulant systematics
Low-Energy Challenges	Space charge, baryon stopping, curlers	Same energy regime challenges	**STAR's BES solutions are prototypes for NICA operations**

Critical point search

B. Mohanty, N. Xu, arXiv:2101.09210

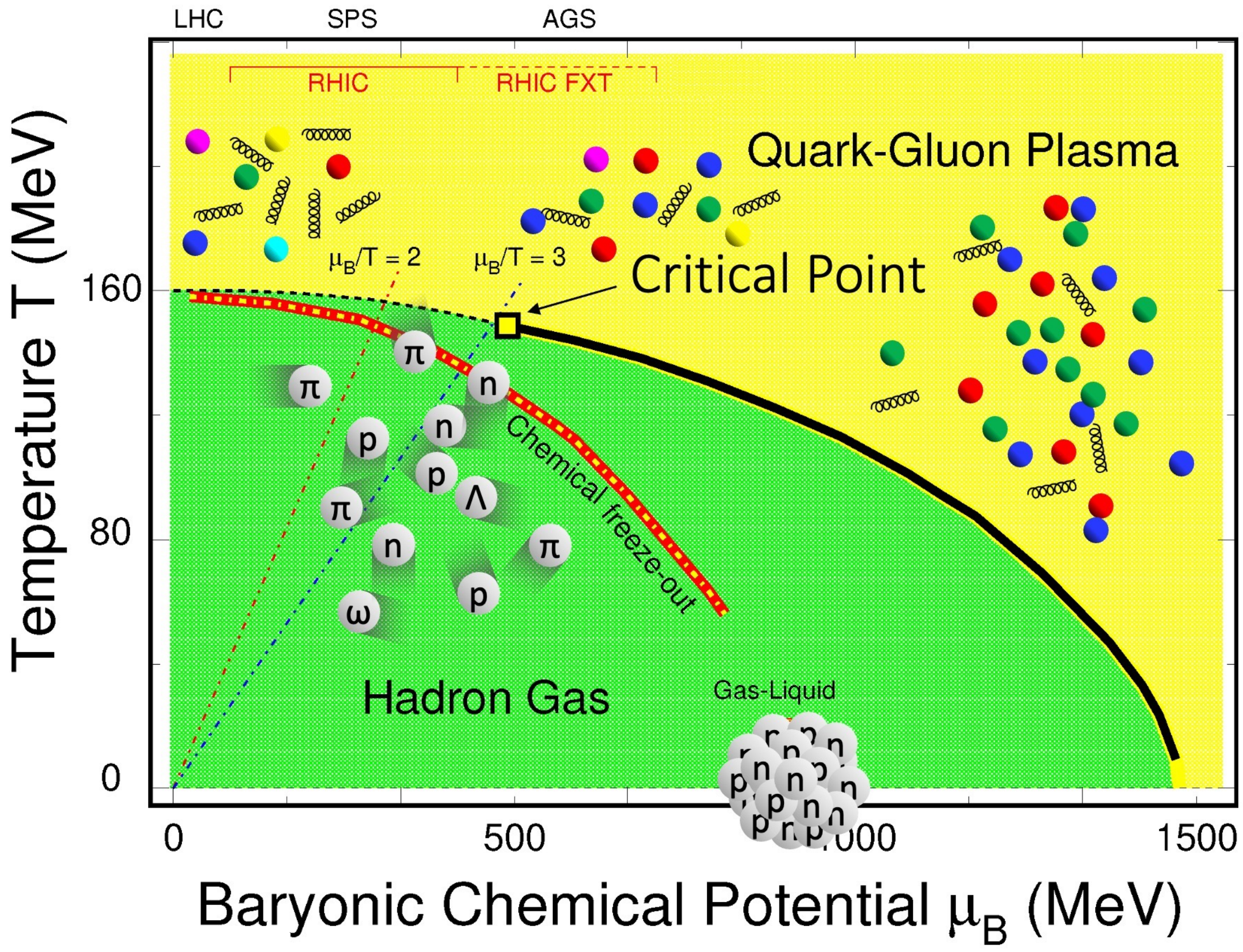

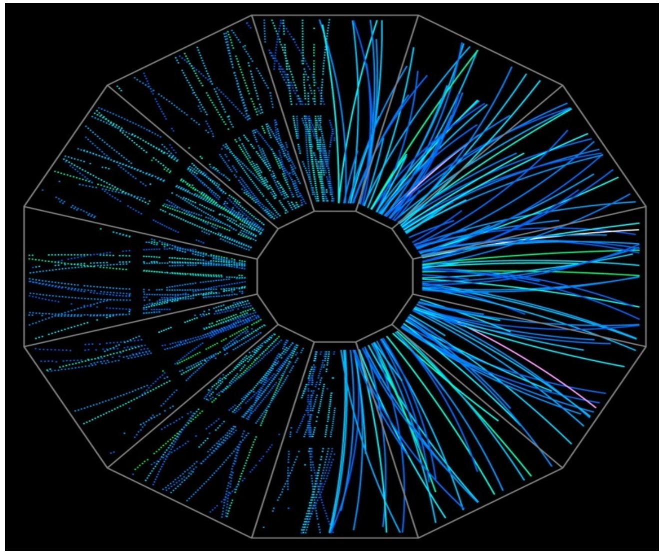

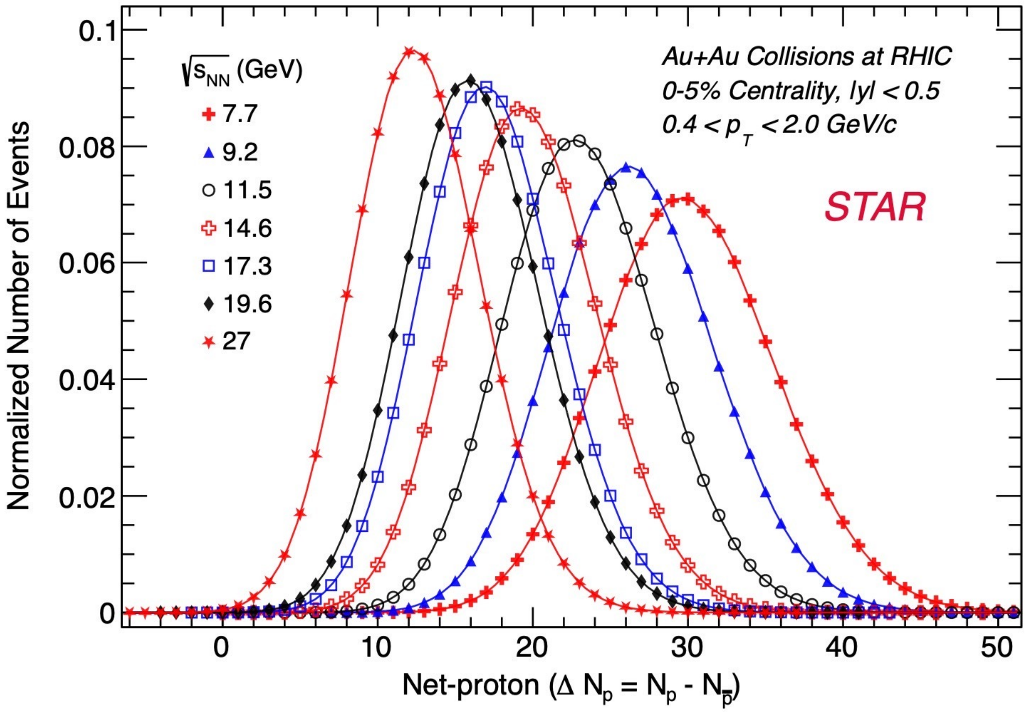

Critical point search: Observable

$$C_1 = \langle N \rangle \equiv \mu \text{ [mean]}$$

$$C_2 = \langle (N-\mu)^2 \rangle \equiv \sigma^2 \text{ [variance]}$$

$$C_3 = \langle (N-\mu)^3 \rangle$$

[related to skewness]

$$C_4 = \langle (N-\mu)^4 \rangle - 3\langle (N-\mu)^2 \rangle^2$$

[related to kurtosis]

$$S\sigma = C_3/C_2$$

$$\kappa\sigma^2 = C_4/C_2$$

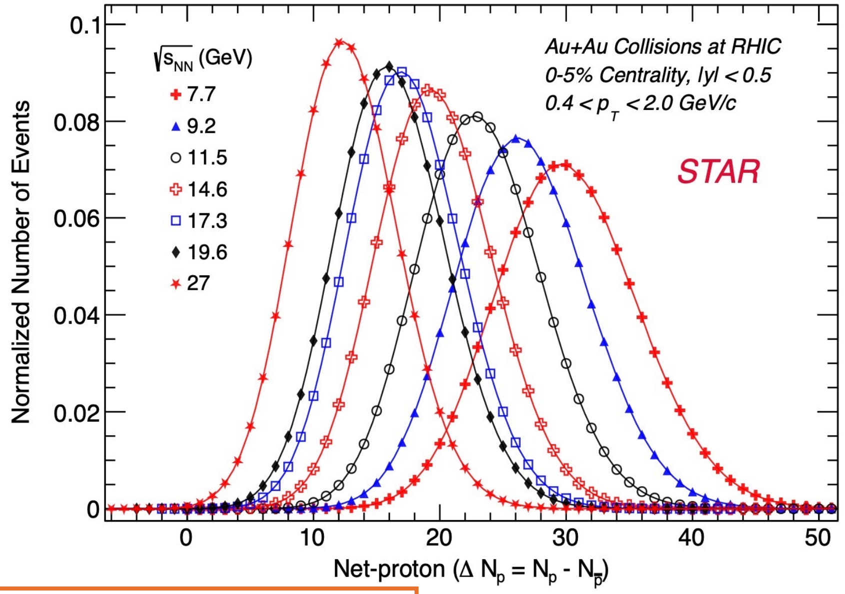

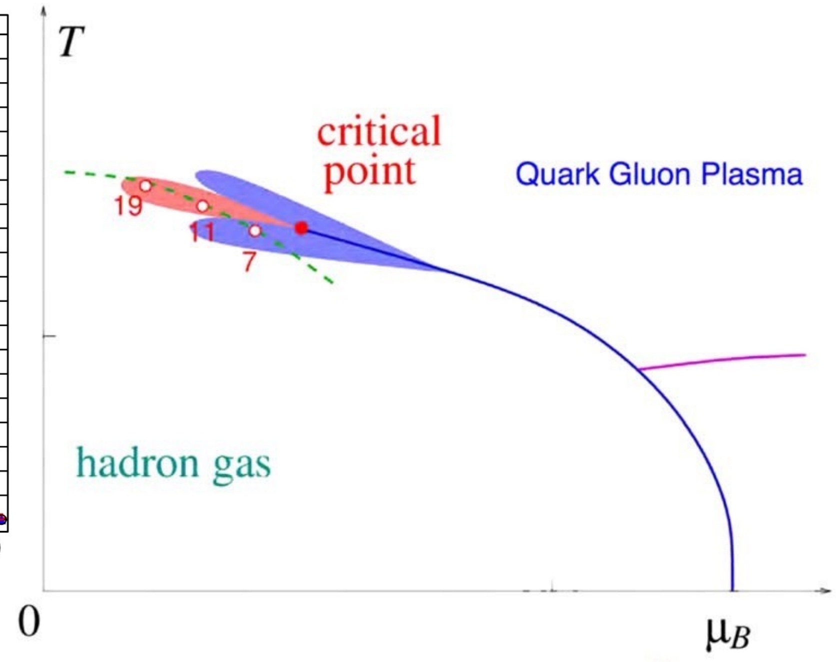

M. Stephanov. J. Physics G.: Nucl. Part. Phys. **38** (2011) 124147

- $C_2 \sim \xi^2$ $\quad C_4 \sim \xi^7$
- $\frac{\chi_q^{(4)}}{\chi_q^{(2)}} = \kappa\sigma^2 = \frac{C_{4,q}}{C_{2,q}}$ $\quad \frac{\chi_q^{(3)}}{\chi_q^{(2)}} = S\sigma = \frac{C_{3,q}}{C_{2,q}}$

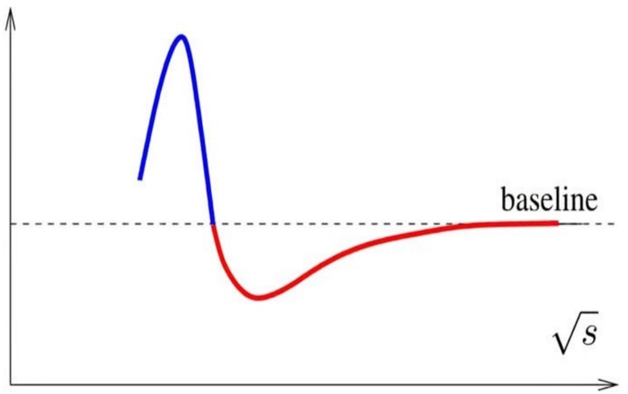

1. Distribution of net-baryon number is expected to fluctuate near a critical point, leading to a non-monotonic variation of fourth order fluctuations with collision energy
2. Experimentally net-protons(N_p-N_{pbar}) are proxies for net-baryon number.

Critical point search: BES-I results

Published results

C_4/C_2

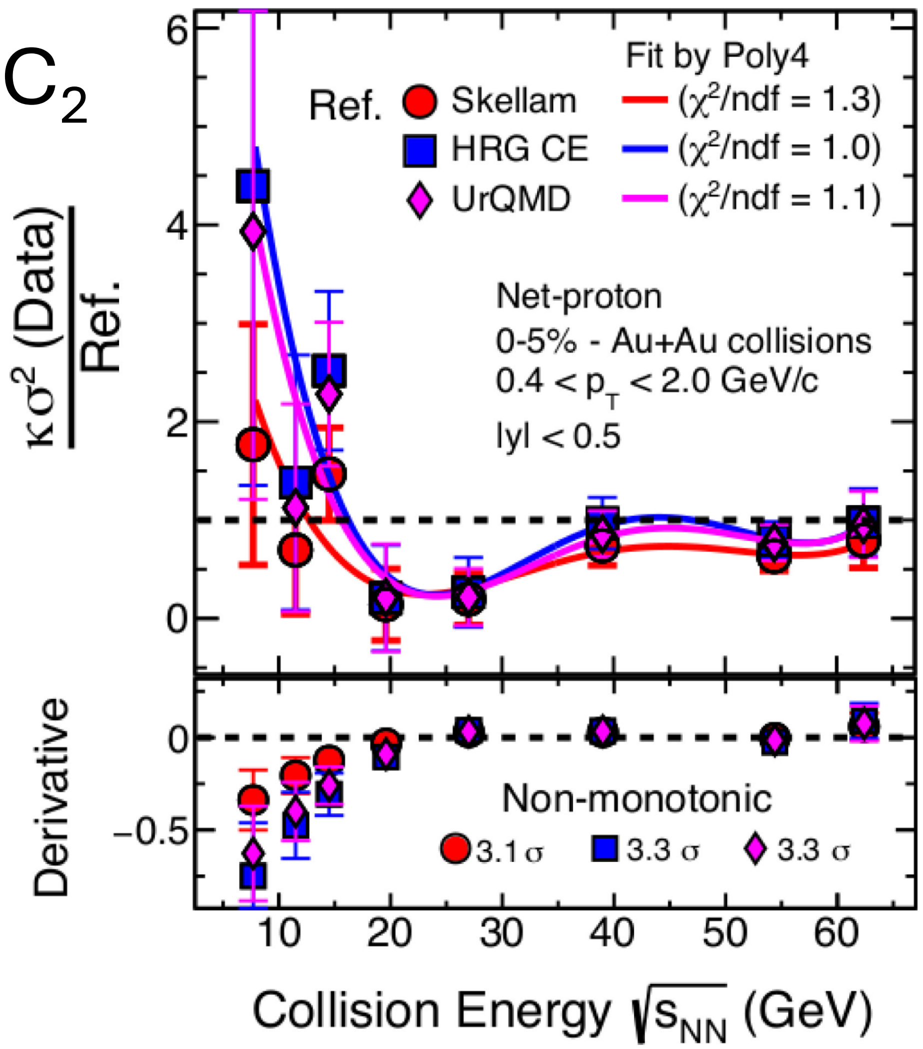

STAR, Phys. Rev. Lett. 128, 202303 (2022); Phys.Rev.C 107.024908 (2023).
Phys. Rev. Lett. 126, 092301 (2021); Phys. Rev. C 104, 024902 (2021)

Non monotonic variation of fourth order net-proton (net-baryon number) fluctuations near critical point

M. Stephanov. J. Physics G.: Nucl. Part. Phys. **38** (2011) 124147

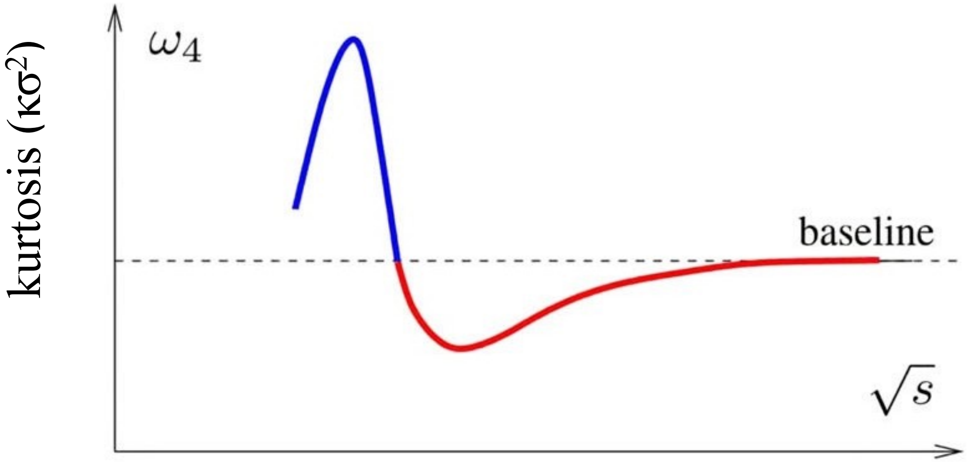

Phase-II

- 10-18-fold increase in statistics
- Two new collision energies
- Detector upgrades in STAR: Better control on centrality resolution and volume fluctuations

QCD critical point search

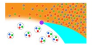

FEATURED IN PHYSICS | EDITORS' SUGGESTION

Precision Measurement of Net-Proton-Number Fluctuations in Au + Au Collisions at RHIC

B. E. Aboona *et al.* (STAR Collaboration)

Phys. Rev. Lett. **135**, 142301 (2025) - Published 29 September, 2025

Experiments at the Relativistic Heavy Ion Collider give the first hints of a critical point in the hot quark–gluon “soup” that is thought to have pervaded the infant Universe.

Hide Abstract

PDF

We report precision measurements on cumulants (C_n) and factorial cumulants (κ_n) of (net) proton number distributions up to fourth order in Au + Au collisions over center-of-mass energies $\sqrt{s_{NN}} = 7.7$–27 GeV from phase II of the Beam Energy Scan program at RHIC. (Anti)protons are selected at midrapidity ($|y| < 0.5$) within a transverse momentum range of $0.4 < p_T < 2.0$ GeV$/c$. Relative to various noncritical-point model calculations and peripheral collision 70%–80% data, the net proton C_4/C_2 measurement in 0%–5% collisions shows a minimum around 19.6 GeV for significance of deviation at ~ 2–5σ. A minimum in C_4/C_2 with respect to a noncritical baseline is expected to be a characteristic feature of the signature associated with a critical point in the QCD phase diagram. In addition, deviations from noncritical baselines around the same collision energy region are also seen in proton factorial cumulant ratios, especially in κ_2/κ_1 and κ_3/κ_1. Dynamical model calculations including a critical point are called for in order to understand these precision measurements.

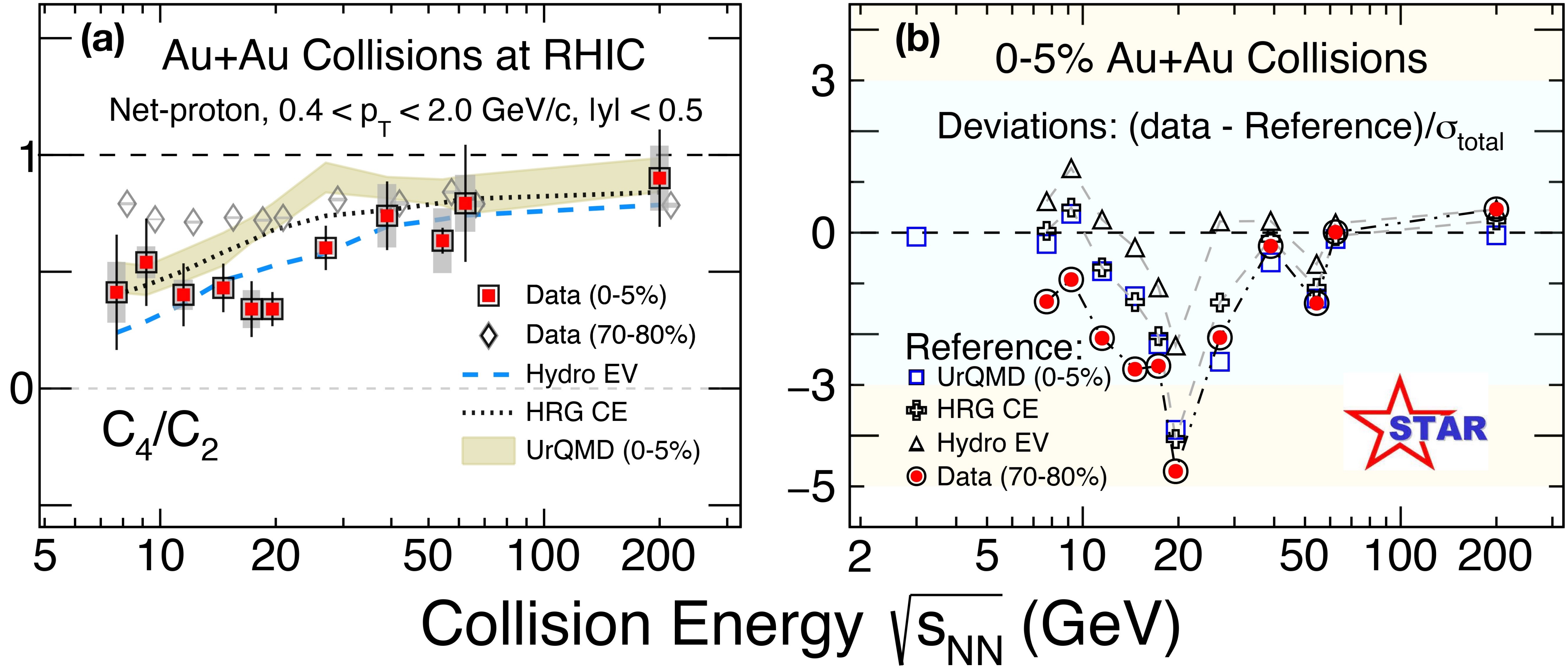

STAR: PRL 135, 142301 (2025)

Establishing the QCD critical point

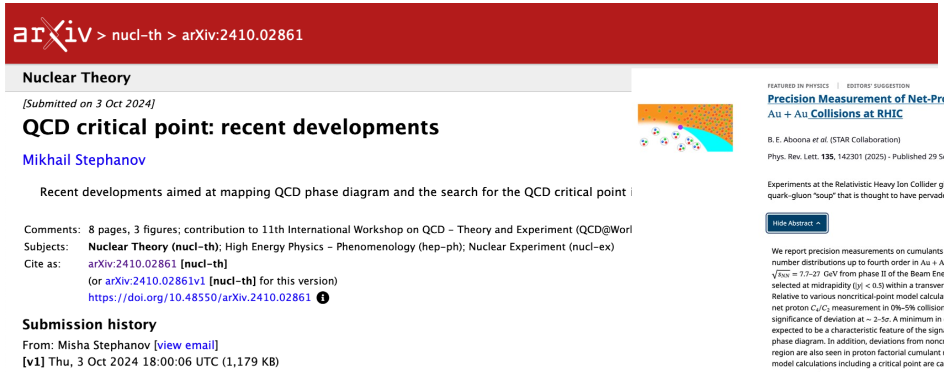
arXiv > nucl-th > arXiv:2410.02861

Nuclear Theory

[Submitted on 3 Oct 2024]

QCD critical point: recent developments

Mikhail Stephanov

Recent developments aimed at mapping QCD phase diagram and the search for the QCD critical point

Comments: 8 pages, 3 figures; contribution to 11th International Workshop on QCD – Theory and Experiment (QCD@Worl

Subjects: **Nuclear Theory (nucl-th)**; High Energy Physics – Phenomenology (hep-ph); Nuclear Experiment (nucl-ex)

Cite as: arXiv:2410.02861 **[nucl-th]**

(or arXiv:2410.02861v1 **[nucl-th]** for this version)

https://doi.org/10.48550/arXiv.2410.02861

Submission history

From: Misha Stephanov [view email]

[v1] Thu, 3 Oct 2024 18:00:06 UTC (1,179 KB)

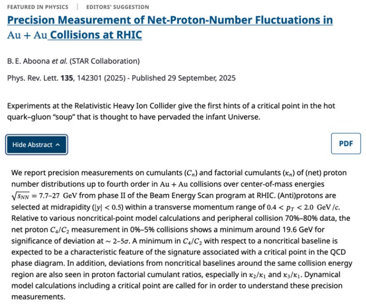
FEATURED IN PHYSICS | EDITORS' SUGGESTION

Precision Measurement of Net-Proton-Number Fluctuations in Au + Au Collisions at RHIC

B. E. Aboona *et al.* (STAR Collaboration)

Phys. Rev. Lett. **135**, 142301 (2025) - Published 29 September, 2025

Experiments at the Relativistic Heavy Ion Collider give the first hints of a critical point in the hot quark–gluon "soup" that is thought to have pervaded the infant Universe.

Hide Abstract

PDF

We report precision measurements on cumulants (C_n) and factorial cumulants (κ_n) of (net) proton number distributions up to fourth order in Au + Au collisions over center-of-mass energies $\sqrt{s_{NN}} = 7.7$–27 GeV from phase II of the Beam Energy Scan program at RHIC. (Anti)protons are selected at midrapidity ($|y| < 0.5$) within a transverse momentum range of $0.4 < p_T < 2.0$ GeV/c. Relative to various noncritical-point model calculations and peripheral collision 70%–80% data, the net proton C_4/C_2 measurement in 0%–5% collisions shows a minimum around 19.6 GeV for significance of deviation at ~ 2–5σ. A minimum in C_4/C_2 with respect to a noncritical baseline is expected to be a characteristic feature of the signature associated with a critical point in the QCD phase diagram. In addition, deviations from noncritical baselines around the same collision energy region are also seen in proton factorial cumulant ratios, especially in κ_2/κ_1 and κ_3/κ_1. Dynamical model calculations including a critical point are called for in order to understand these precision measurements.

CP based model in qualitative agreement with measurements

Caveats

1. Choice of the baseline
2. Based on Ising model (singular & regular)
3. Does not tell the location of CP

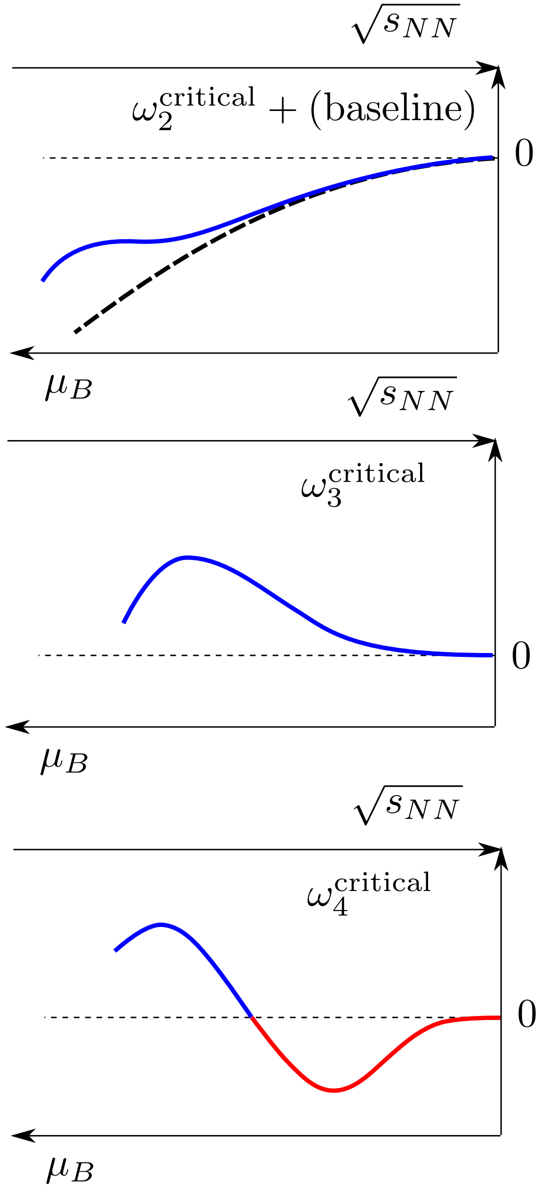

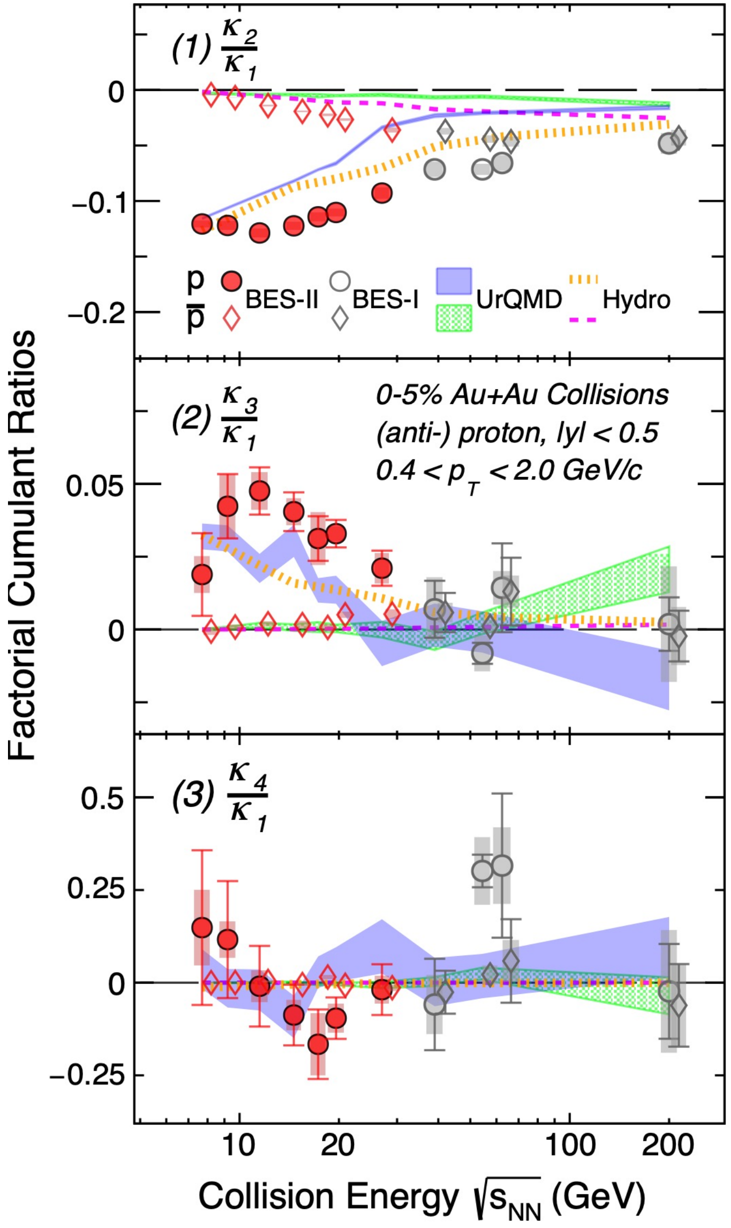

Critical point search: BES-I + II

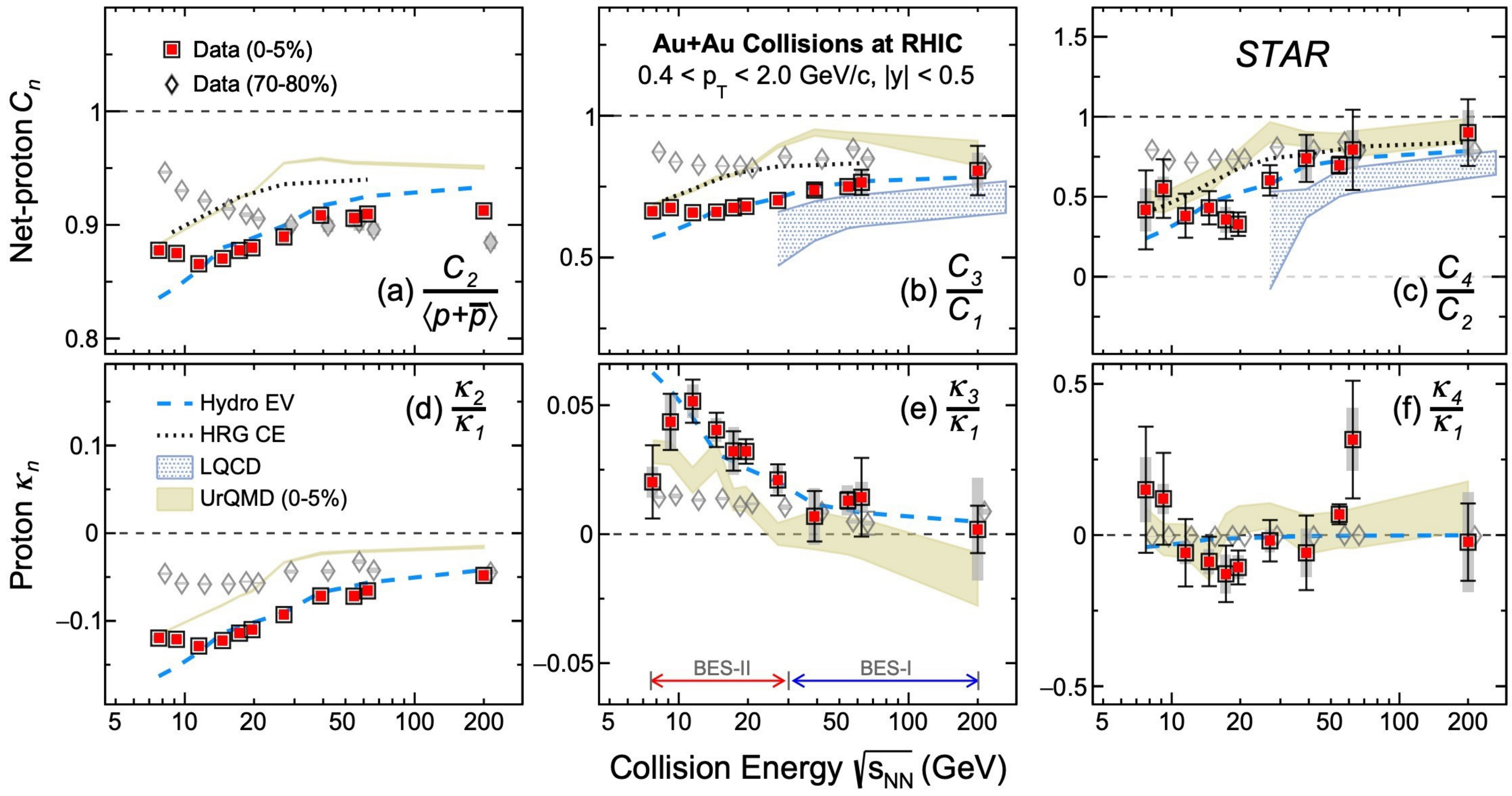

STAR: PRL 135, 142301 (2025)

Critical point search: BES-I + II results + Fixed target

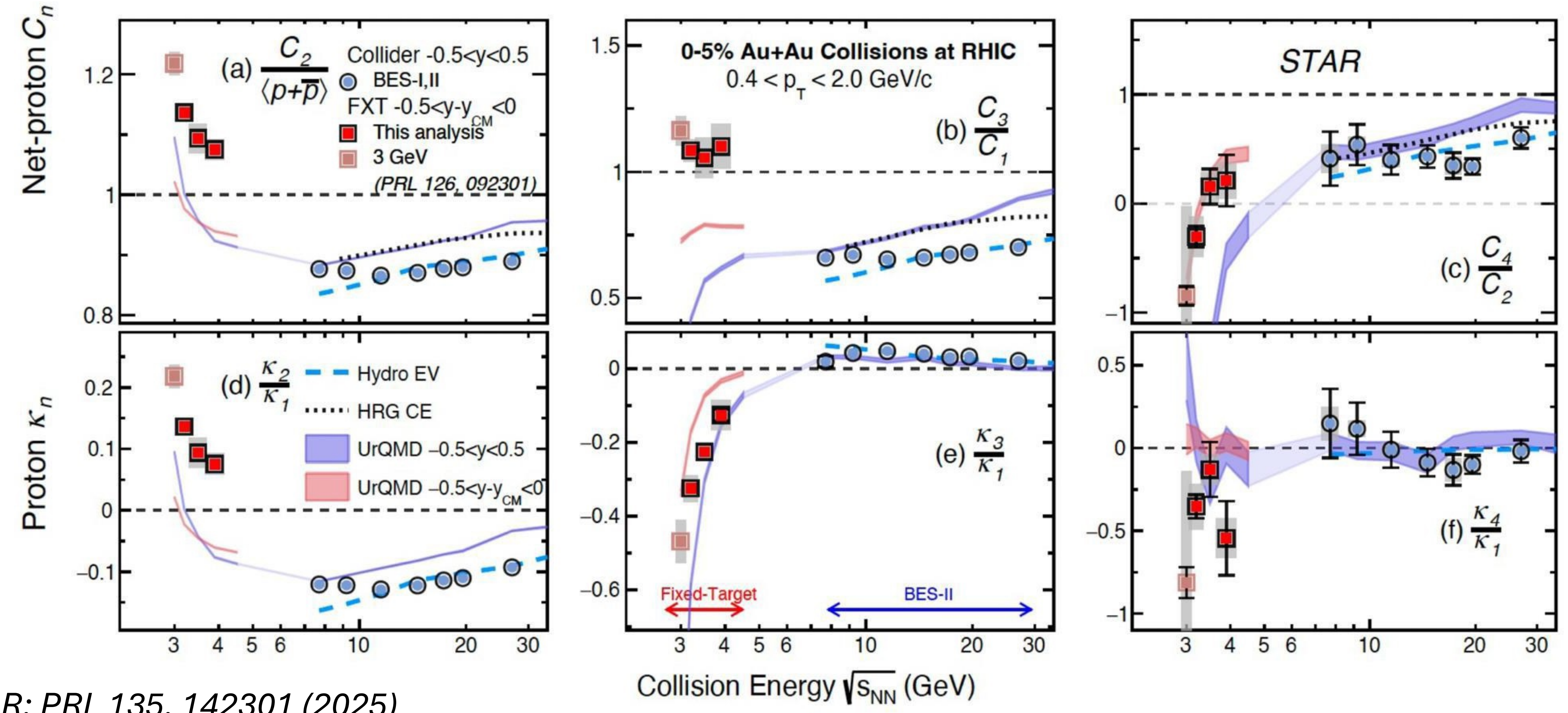

STAR: PRL 135, 142301 (2025)

Significant deviations from non-critical baseline

Critical point search: need continued program at high baryon density

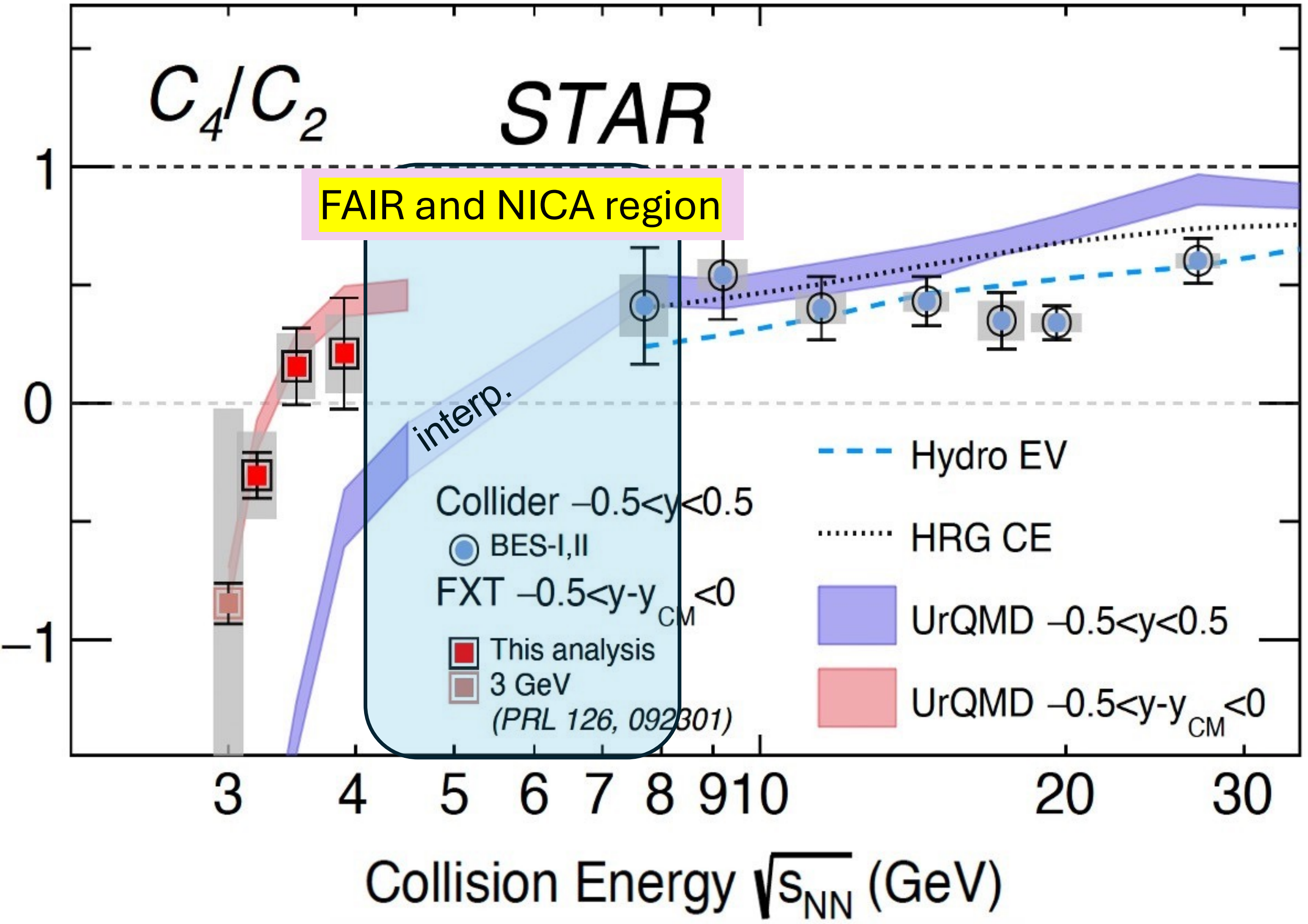

STAR: PRL 135, 142301 (2025)

arXiv:2410.16206 [hep-ph]

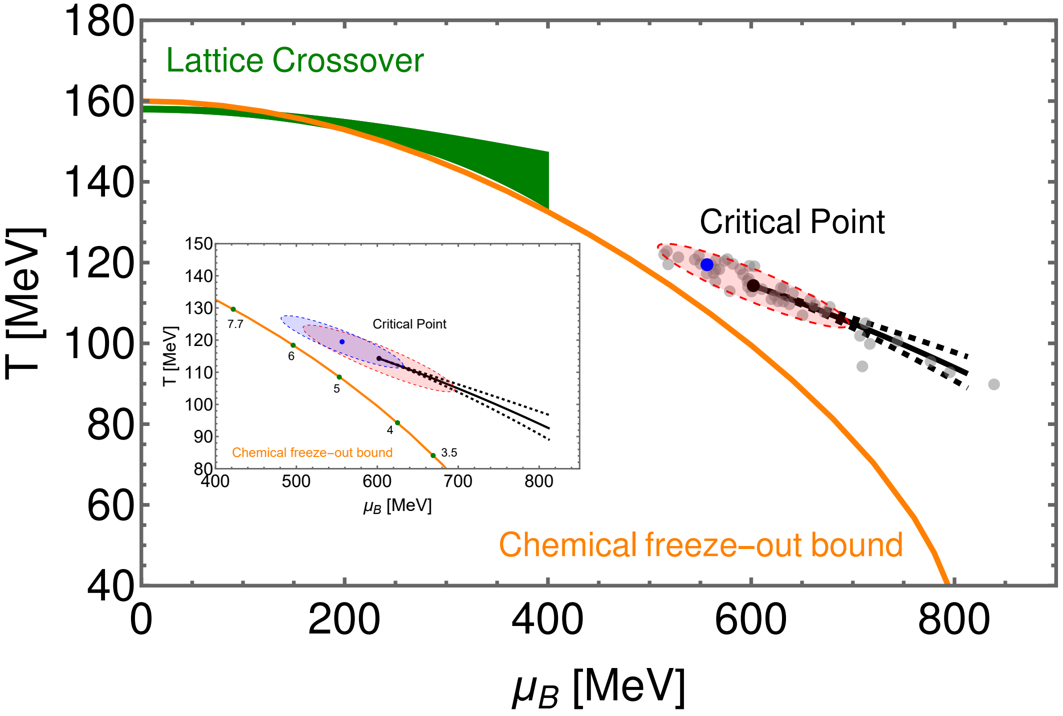

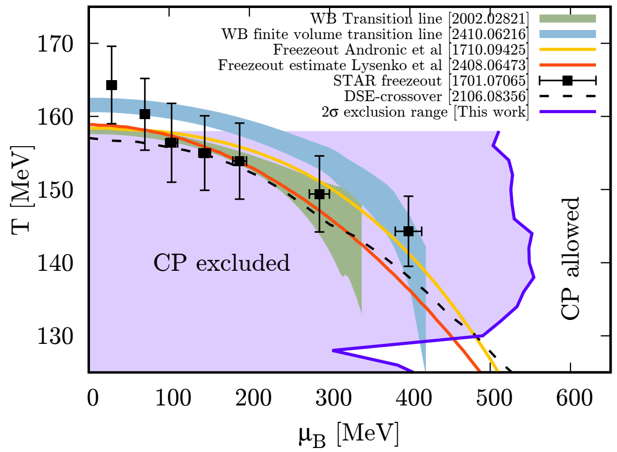

Szabolcs Borsanyi, arXiv:2502.10267

Summary on critical point search

1. Interesting trends in STAR BES data
2. Trends consistent with a model with critical point. Could be due to system passing through critical region.
3. Real critical point location now theory expects to be around μ_B 400 – 700 MeV
4. RHIC closes down in March 2026. Need to continue this program at CBM-FAIR and MPD-NICA-JINR.

Prog.Part.Nucl.Phys. 125 (2022) 103960

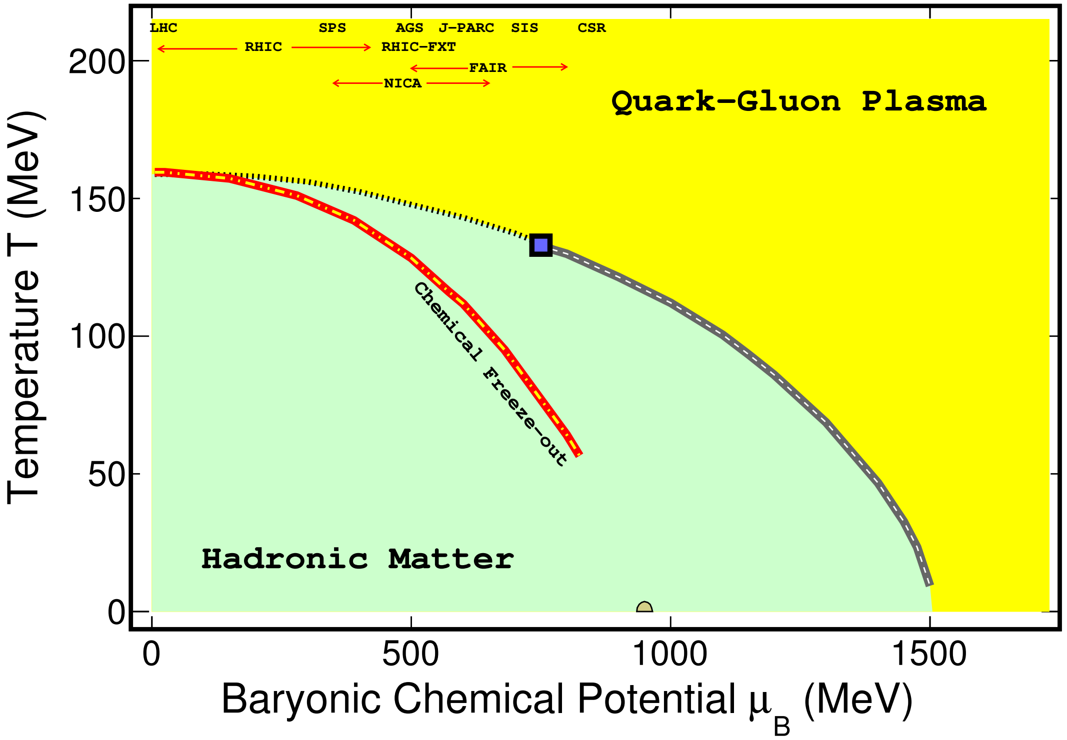

Large angular momentum (1)

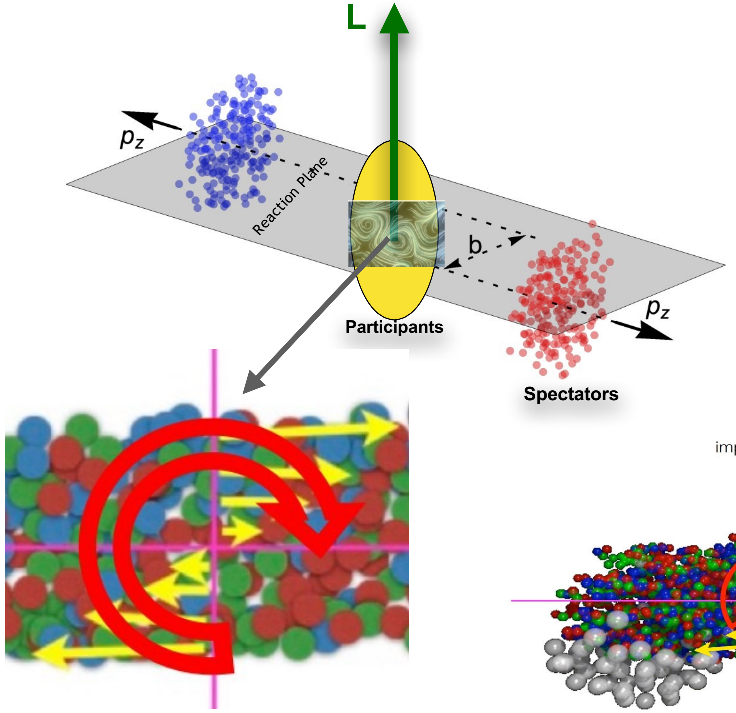

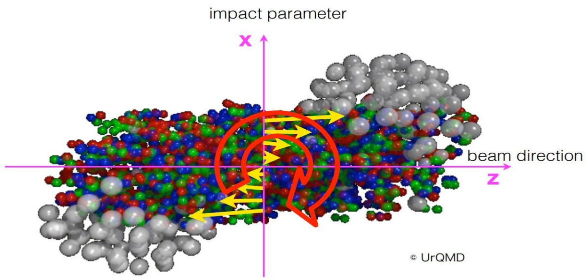

Vorticity generation

$$L = r \times p \sim bA\sqrt{s_{\mathrm{NN}}} \sim 10^4\,\hbar$$

$$\omega = \frac{1}{2}\nabla \times v \qquad \omega_y = \frac{1}{2}(\nabla \times v)_y \approx \frac{1}{2}\frac{dv_z}{dy}$$

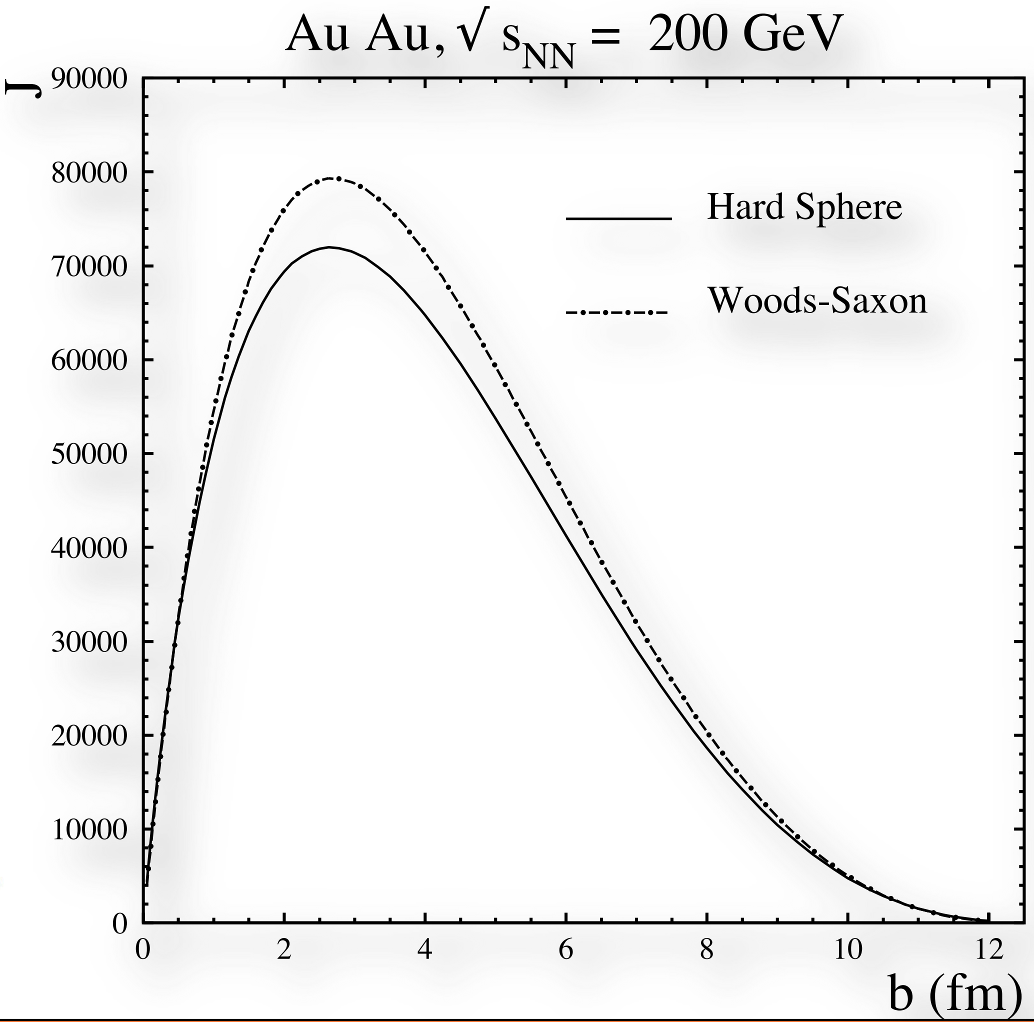

F. Becattini et al., Phys.Rev.C 77 (2008) 024906

- Angular momentum conserved quantity
- Spin-orbital angular momentum interactions – Polarization of hyperons and spin alignment of vector mesons

Large angular momentum (2)

Vector meson spin alignment

$$\frac{dN}{dcos\theta} = N_0\left[1-\rho_{0,0}+cos^2\theta\,(3\rho_{0,0}-1)\right]$$

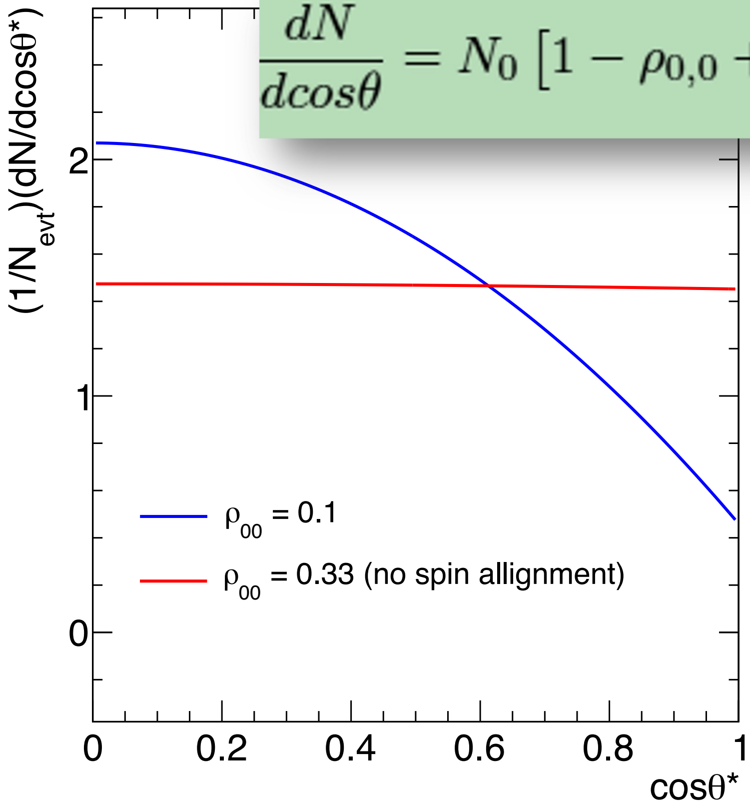

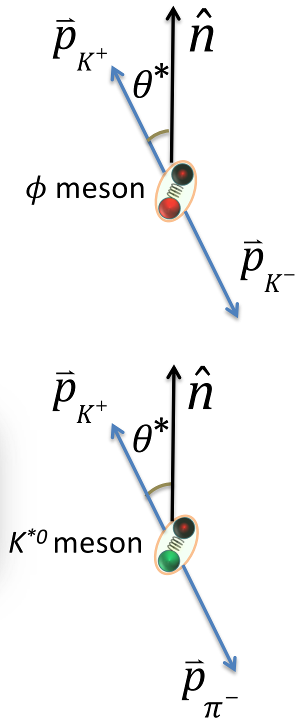

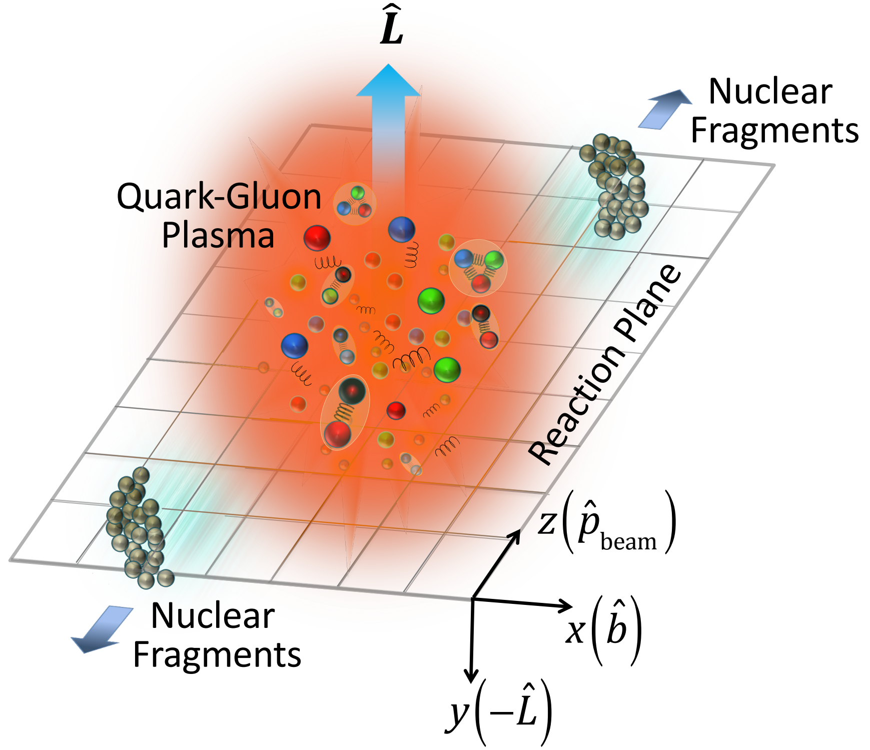

How does on experimentally access spin alignment or polarization?
Study angular distribution of decay products of a hyperon or a vector meson.

Large angular momentum (3)

ALICE: K* meson spin alignment – 3σ effect

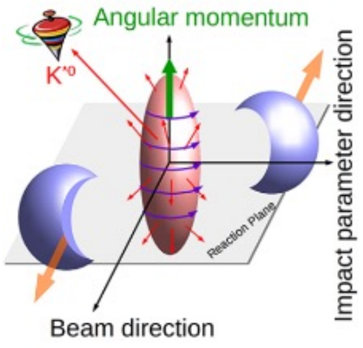

EDITORS' SUGGESTION

Evidence of Spin-Orbital Angular Momentum Interactions in Relativistic Heavy-Ion Collisions

The measured spin alignment of vector mesons in heavy-ion collisions is consistent with that expected from the spin-orbit coupling of quarks with the large angular momentum of the collision.

S. Acharya *et al.* (The ALICE Collaboration)
Phys. Rev. Lett. **125**, 012301 (2020)

$$\frac{dN}{dcos\theta} = N_0\left[1-\rho_{0,0}+cos^2\theta\,(3\rho_{0,0}-1)\right]$$

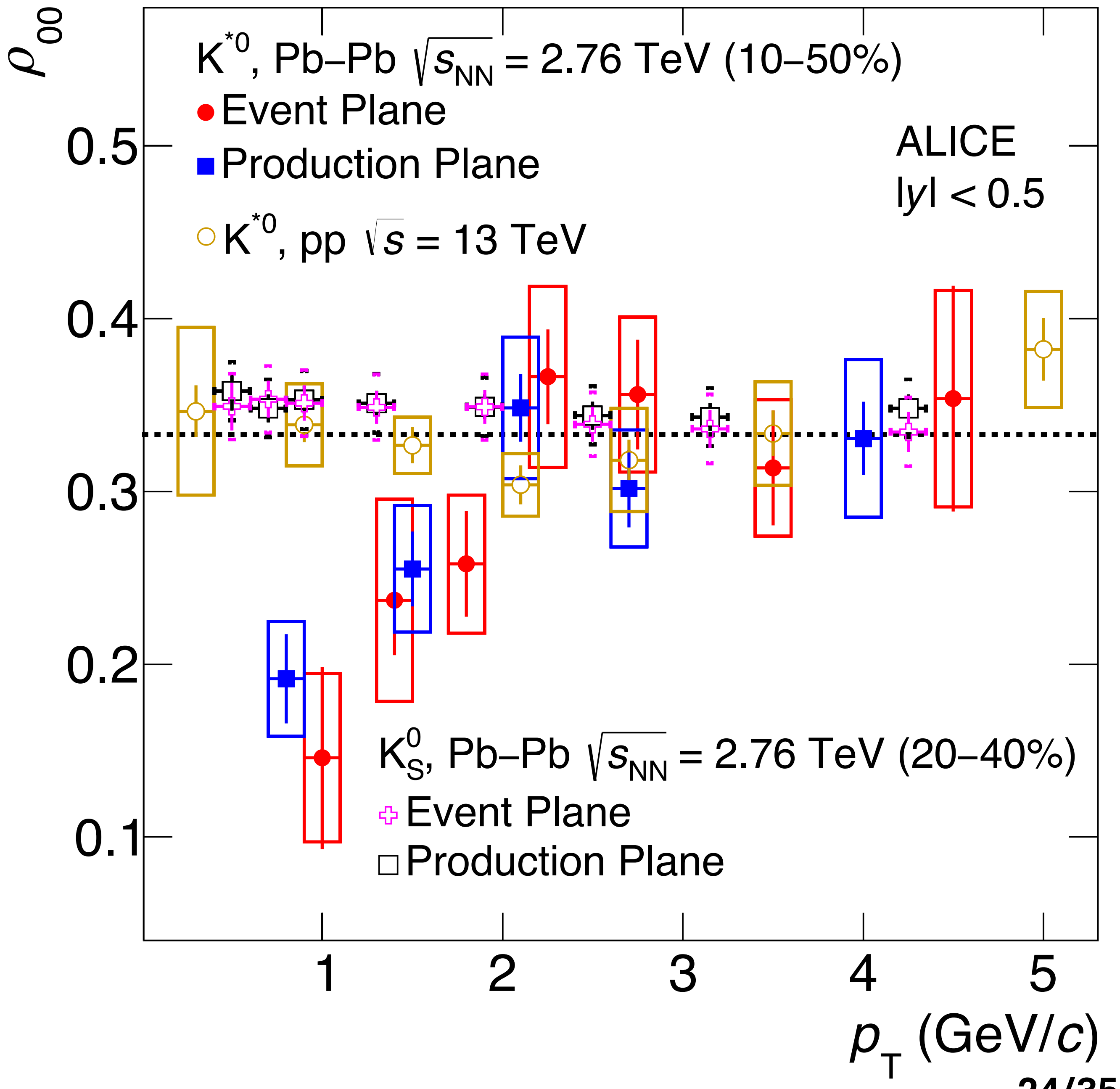

Large angular momentum (4)

STAR: ϕ meson spin alignment – 8σ effect

nature

Explore content ⌄ About the journal ⌄ Publish with us ⌄

nature › articles › article

Article | Published: 18 January 2023

Pattern of global spin alignment of φ and K^{*0} mesons in heavy-ion collisions

STAR Collaboration

Nature **614**, 244–248 (2023) | Cite this article

$$\frac{dN}{dcos\theta} = N_0\left[1 - \rho_{0,0} + cos^2\theta\,(3\rho_{0,0} - 1)\right]$$

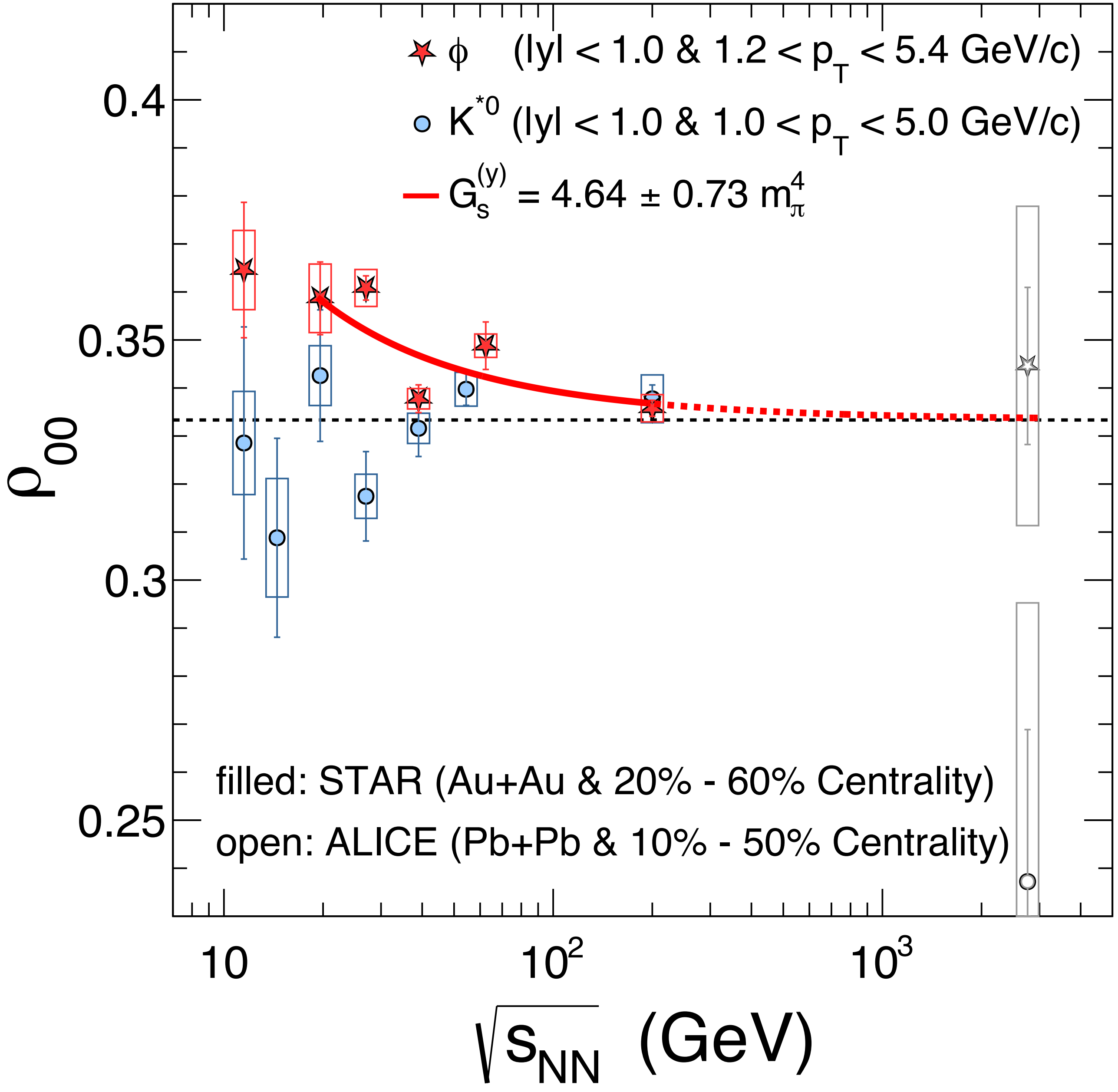

Large angular momentum (5)

ALICE: J/ψ meson spin alignment – 3.5σ effect (forward rapidity)

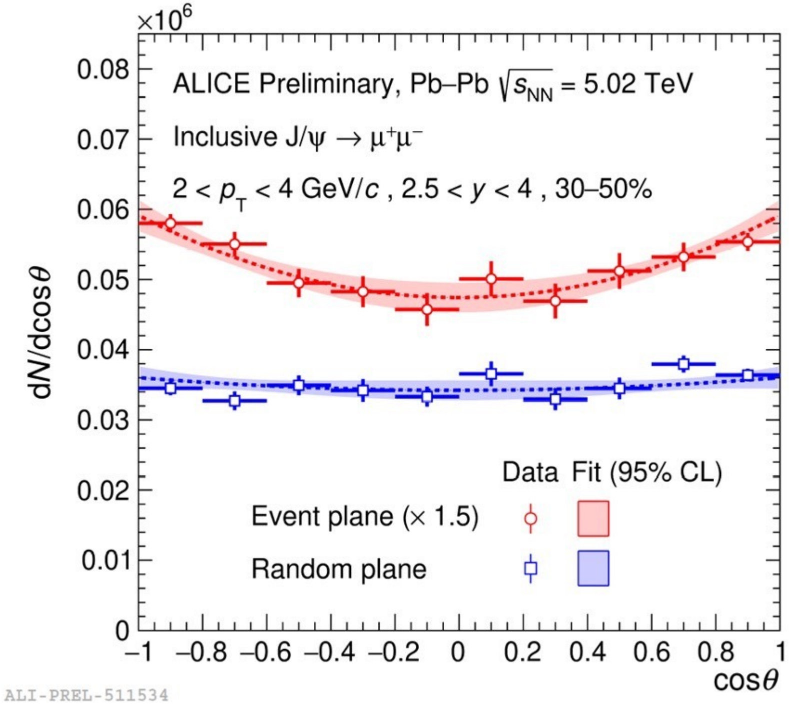

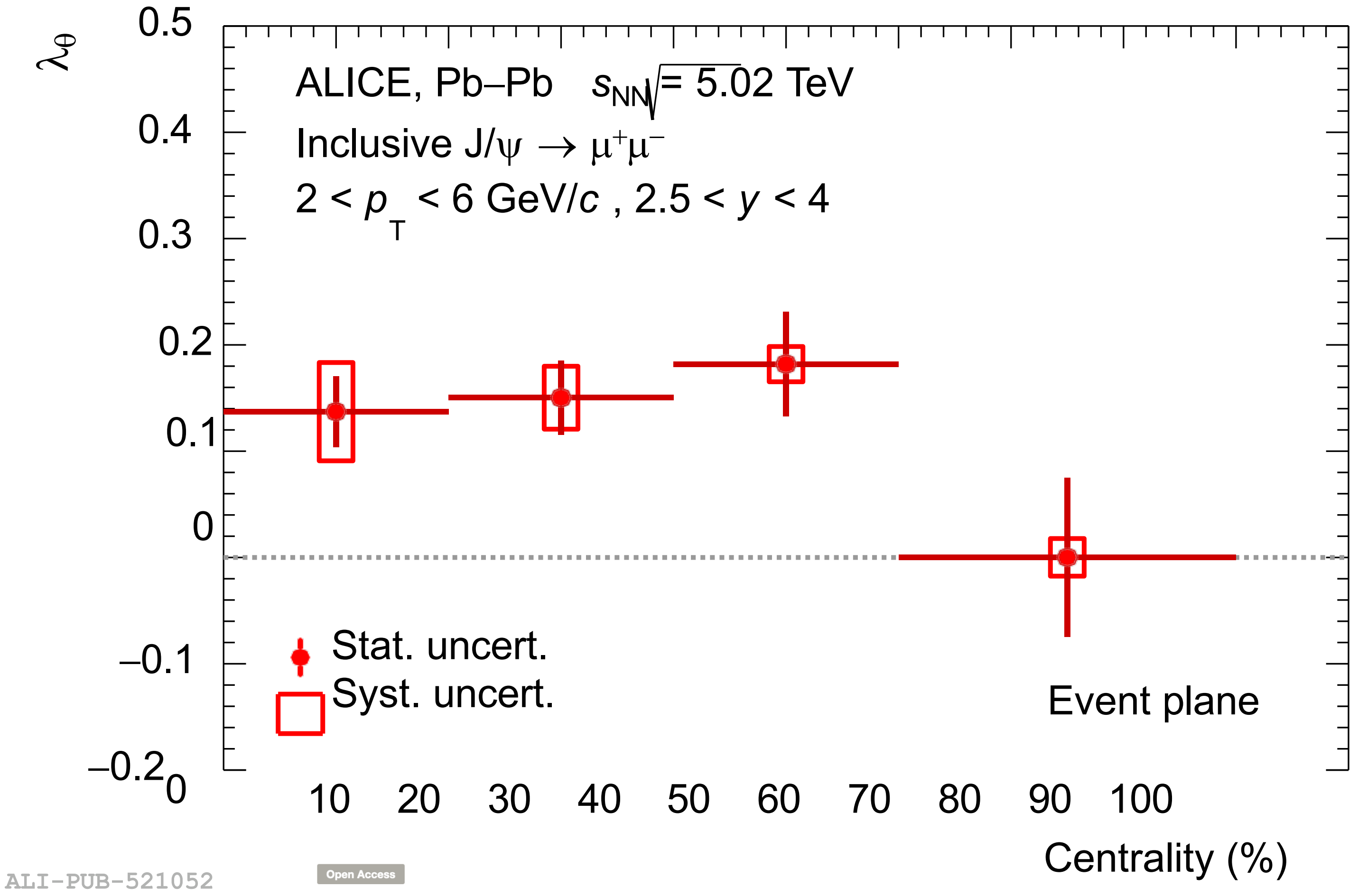

- In the dilepton channel:

$$\lambda_\theta = \frac{1 - 3\rho_{00}}{1 + \rho_{00}}$$

$\lambda_\theta > 0 \rightarrow \rho_{00} < 1/3$

$\lambda_\theta < 0 \rightarrow \rho_{00} > 1/3$

Open Access
Measurement of the J/ψ Polarization with Respect to the Event Plane in Pb-Pb Collisions at the LHC
S. Acharya *et al.* (ALICE Collaboration)
Phys. Rev. Lett. **131**, 042303 – Published 25 July 2023

Large angular momentum (6)

ALICE: open charm D^{*+} spin alignment

$\rho_{00} < \frac{1}{3}$ quark recombination at low *momentum*

$\rho_{00} > \frac{1}{3}$ quark fragmentation at high *momentum*

$$\frac{dN}{dcos\theta} = N_0 \left[1 - \rho_{0,0} + cos^2\theta \left(3\rho_{0,0} - 1\right)\right]$$

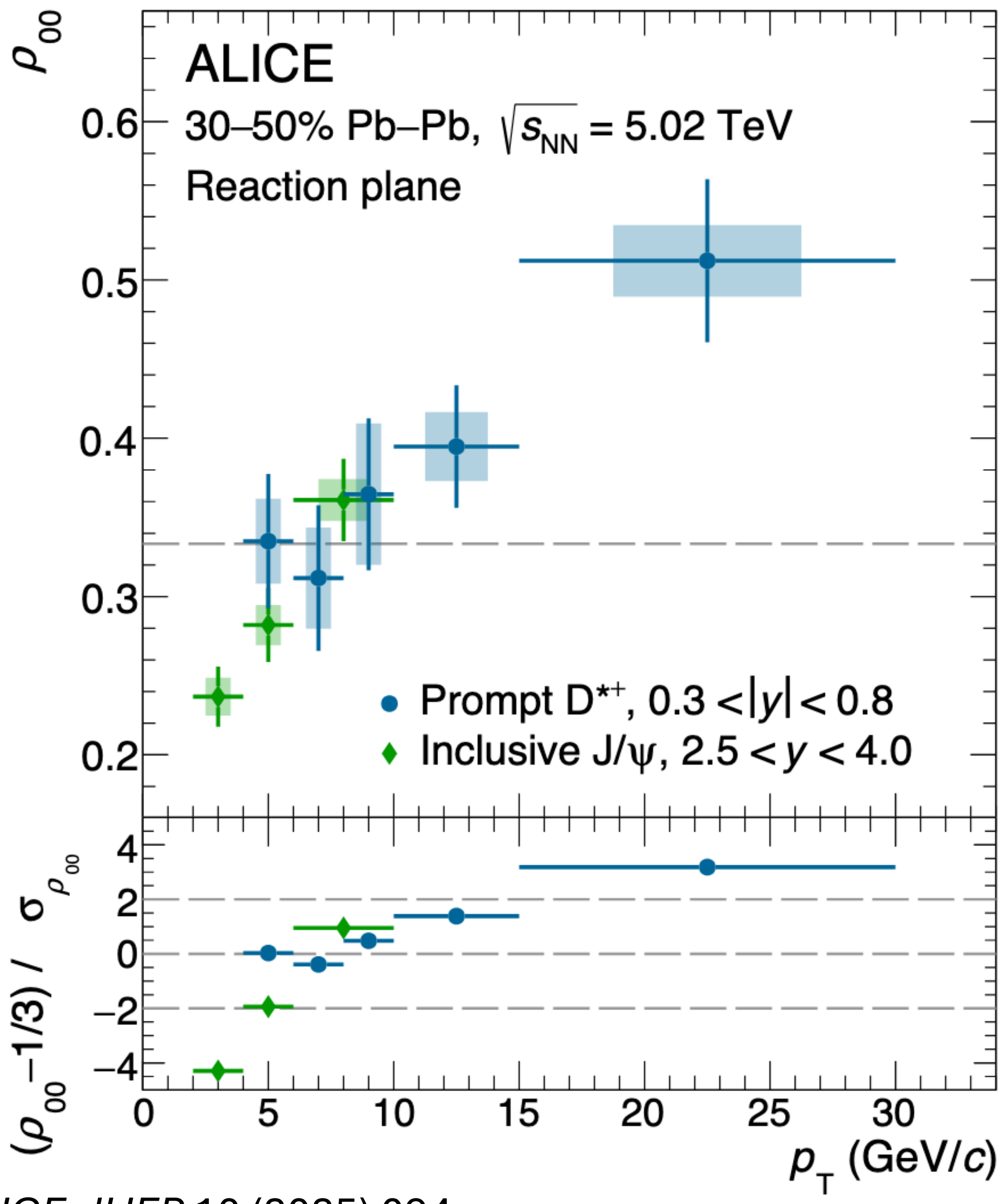

ALICE: JHEP 10 (2025) 094

Large angular momentum (7)

Interesting experimental program on spin alignment unfolding in pp and AA collisions

	K*	ϕ	D*	J/ψ	ψ(2S)	χc	ϒ(nS)
pp	$\rho_{00}\sim 1/3$	$\rho_{00}\sim 1/3$	$\rho_{00}\sim 1/3$	$\rho_{00}\sim 1/3$	$\rho_{00}\sim 1/3$		
Pb-Pb	$\rho_{00} < 1/3$ low p_T	$\rho_{00} < 1/3$ low p_T; $\rho_{00} > 1/3$ At RHIC	$\rho_{00} > 1/3$ high p_T	$\rho_{00} < 1/3$ low p_T			

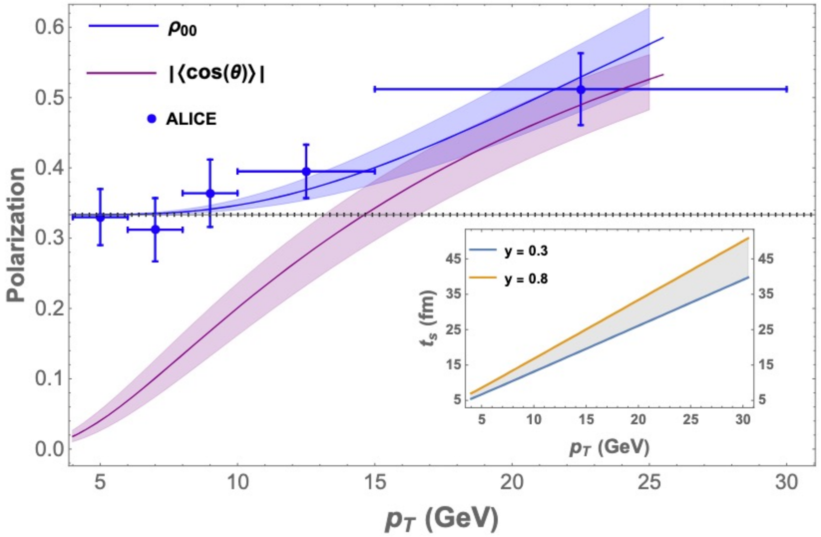

arXiv:2502.20352
Sourav Dey and Amaresh Jaiswal

Theoretical efforts to understand the measurements ongoing. Need for a Spin hydrodynamics development which is happening.

Large angular momentum (8)

Interesting experimental measurements on hyperon polarization

For an ensemble of Λs with polarization $\vec{P}$:

$$\frac{dW}{d\Omega^*} = \frac{1}{4\pi}\left(1+\alpha\vec{P}\cdot\hat{p}_p^*\right) = \frac{1}{4\pi}\left(1+\alpha P\cos\theta^*\right)$$

$\alpha = 0.642$ [measured]

$\hat{p}_p^*$ is the daughter proton momentum direction *in* the Λ *frame*

$$0 < |\vec{P}| < 1: \quad \vec{P} = \frac{3}{\alpha}\bar{\hat{p}}_p^*$$

$$P_\Lambda \approx \frac{1}{2}\frac{\omega}{T} + \frac{\mu_\Lambda B}{T} \qquad P_{\bar{\Lambda}} \approx \frac{1}{2}\frac{\omega}{T} - \frac{\mu_\Lambda B}{T}$$

(for small polarizations)

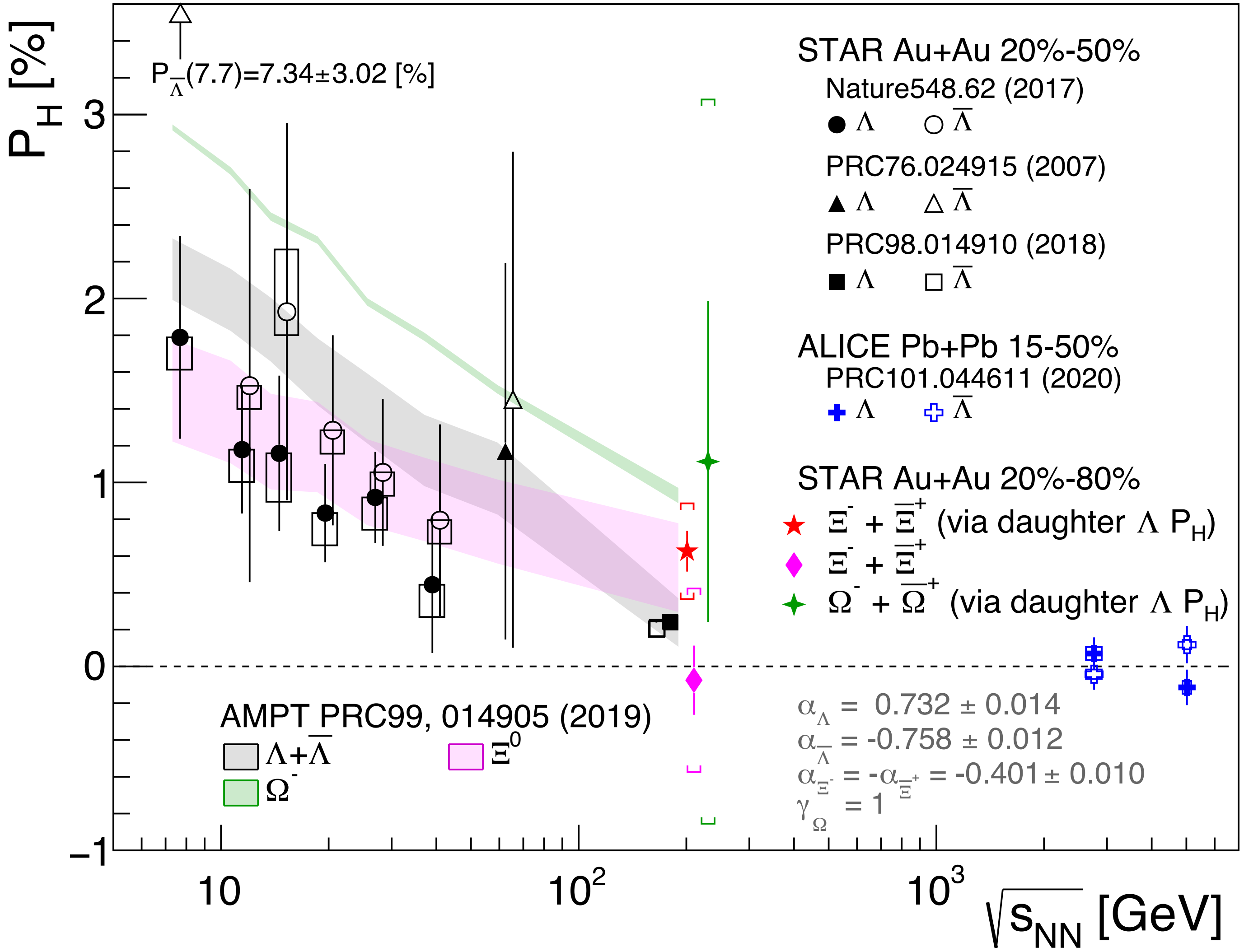

Nature 548, 62 (2017) (STAR Collaboration)
Phys Rev C 98, 14910 (2018) (STAR Collaboration)

Global Polarization of Ξ and Ω Hyperons in Au + Au Collisions at $\sqrt{s_{NN}} = 200$ GeV

J. Adam *et al.* (STAR Collaboration)
Phys. Rev. Lett. **126**, 162301 – Published 22 April 2021; Erratum Phys. Rev. Lett. **131**, 089901 (2023)

Large angular momentum (9)

Hyperon and anti-hyperon polarization: BES-I + II

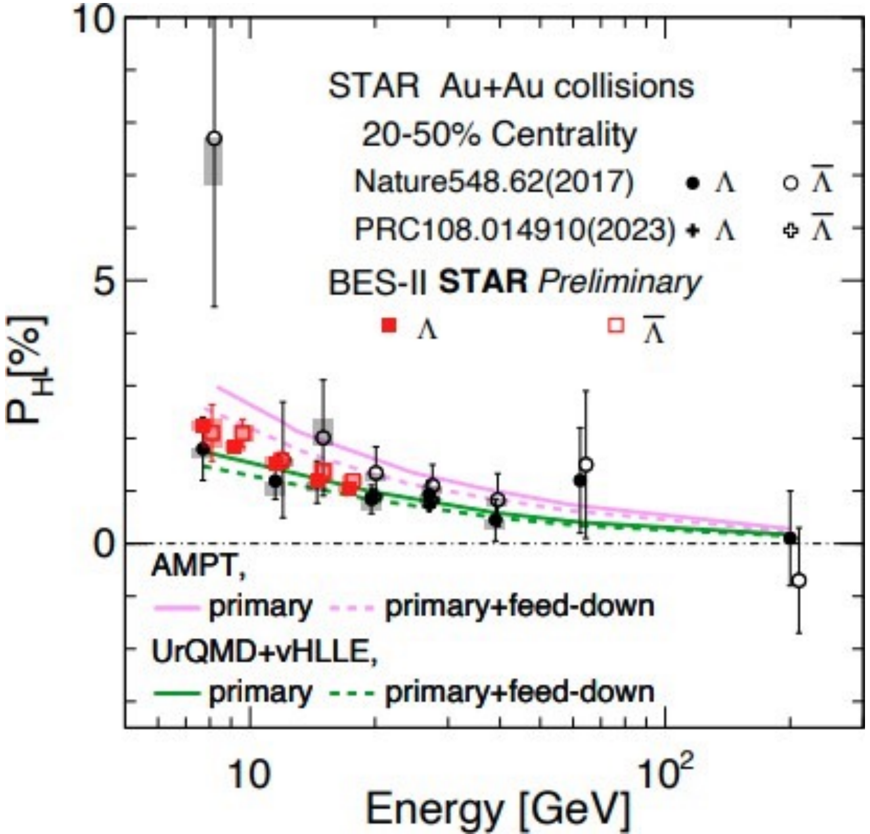

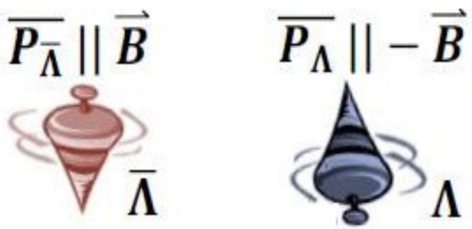

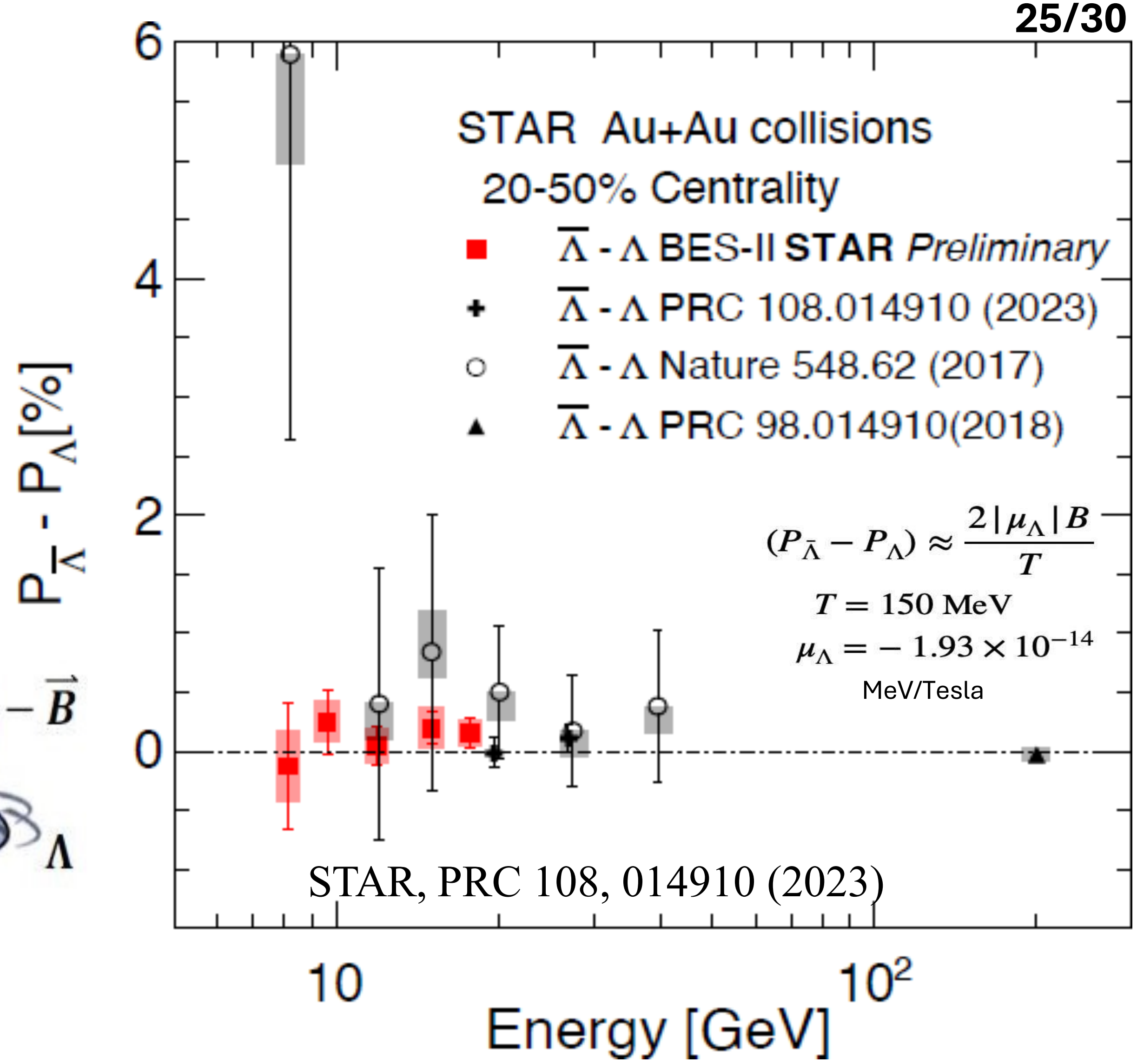

Upper limit on late-stage magnetic field
$B \lesssim 10^{13}$ T (95% confidence level)

Large angular momentum (10)

Λ, Ω, Ξ polarization: BES-I + II

Possible **Λ**, ***Ξ***, **Ω** global polarization difference from different s quark polarization?

Global polarization of Ξ and Ω follows the same trend which was previously established for Λ

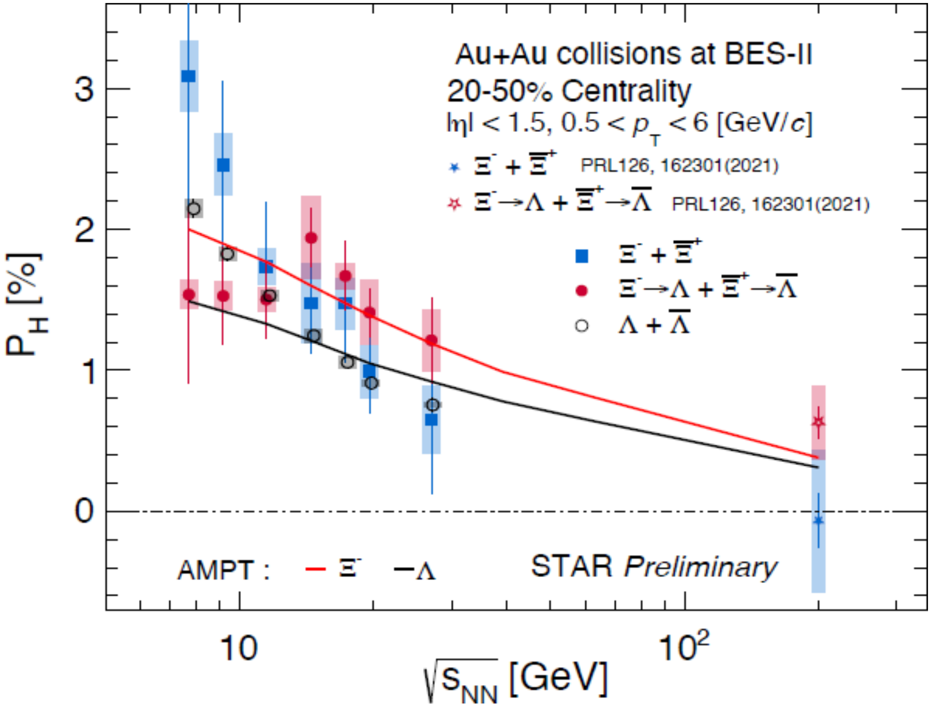

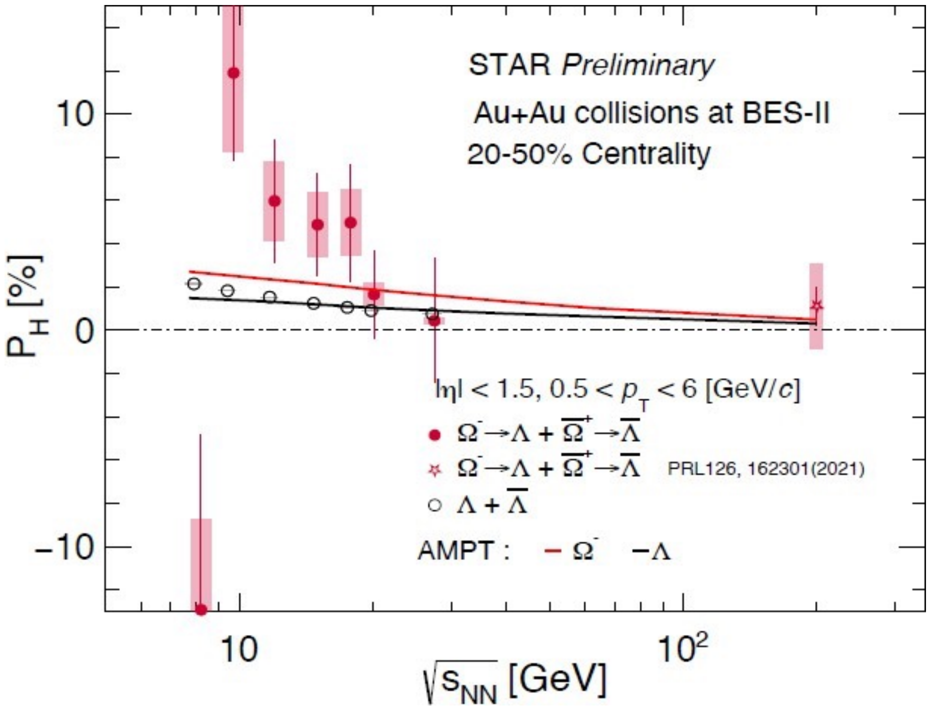

$P_\Lambda \sim P_\Xi \cong P_S$

assuming that

$P_{u,d} \sim P_S$

$$P_\Omega \sim \frac{5}{3} P_\Lambda$$

Z.-T. Liang and X.-N. Wang, PRL 94, 102301 (2005) Hui Li et al., PLB 827, 136971(2022); H. Li, X. Xia et al Phys. Lett. B 827, 136971 (2022)

Large angular momentum (Polarization - global)

Thermal vorticity $\omega = k_B T(P_\Lambda + P_{\bar{\Lambda}})/\hbar$

$\omega \sim (9 \pm 1) \times 10^{21} s^{-1}$

Energy dependence:
Models reproduce data
Effect an interplay of
(a) Shear flow
(b) Baryon stopping
(c) Rapidity acceptance
(d) Lifetime of the system

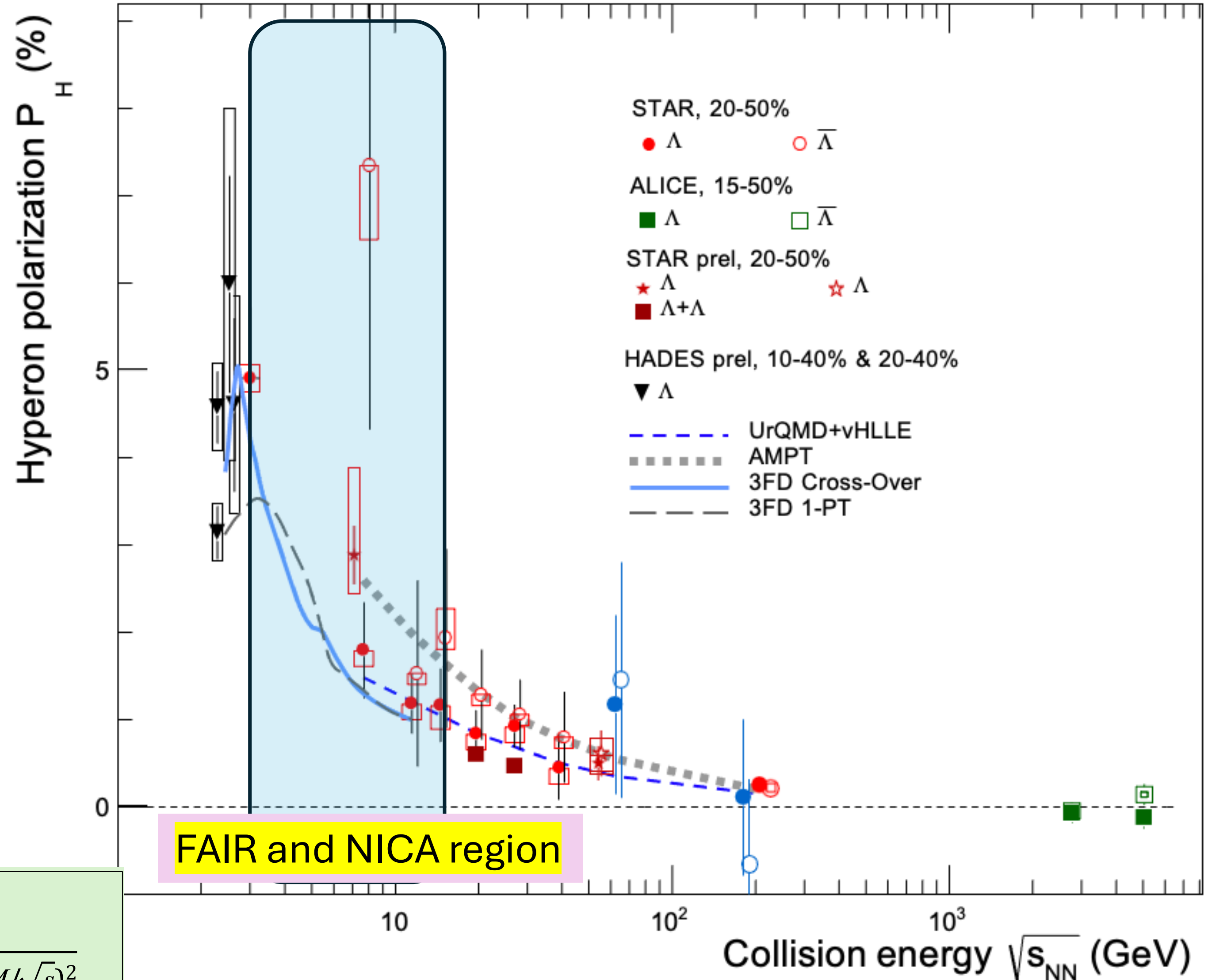

STAR: Phys Rev C 76, 024915 (2007)

Nature 548, 62 (2017)

Becattini, et. al., Phys Rev C 95, 054902 (2017)

Karpenko et. al., Eur Phys J C 77, 213 (2017)

Ivanov et. al., Phys Rev C 100, 014908 (2019)

Ivanov et. al., Phys Rev C 102, 024916 (2020)

Lower energy - Expectation:

$$L \sim \frac{1}{2} A b \sqrt{s} \sqrt{1 - (2M/\sqrt{s})^2}$$

$P_\Lambda \sim 0$ at $\sqrt{s_{NN}} \sim 2m_N$

Models do not capture flat rapidity dependence (not discussed)

EM fields and spin-orbital angular interactions

Experimental program moving fast with new measurements, more differential in nature and better precision.

Theoretical developments need to continue for a relativistic spin-magneto-viscous hydrodynamics to get the complete picture.

Conclusions

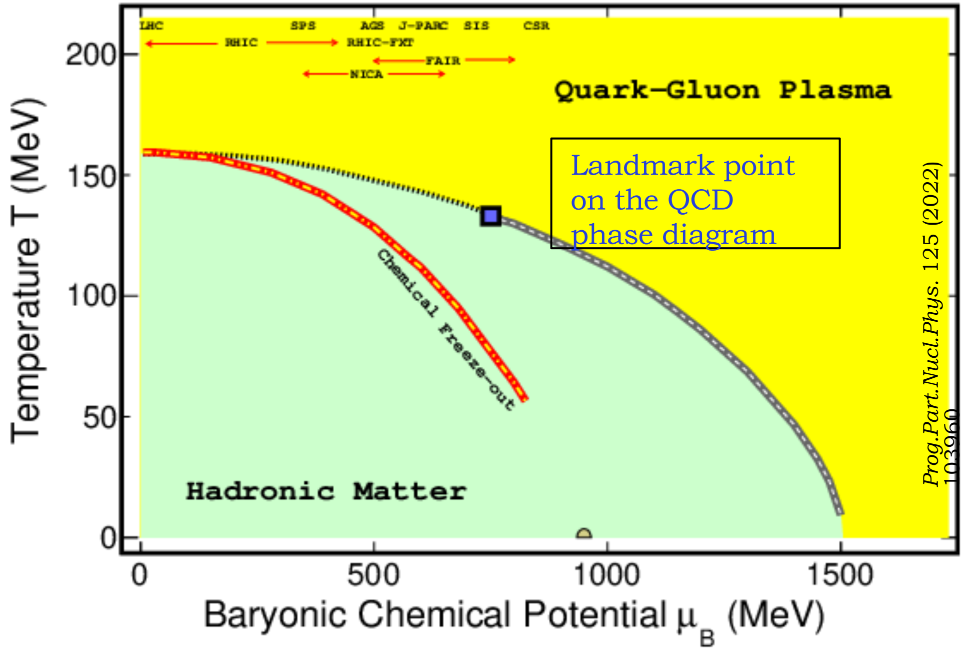

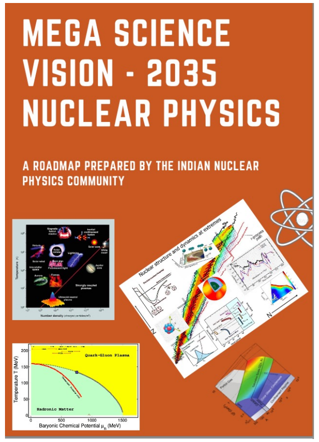

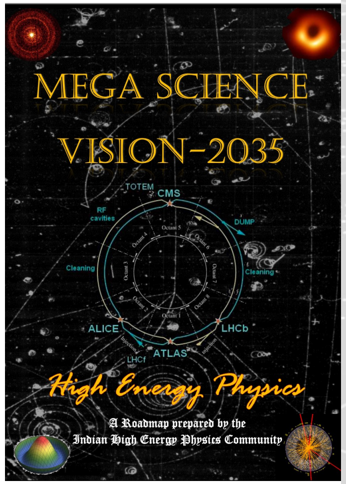

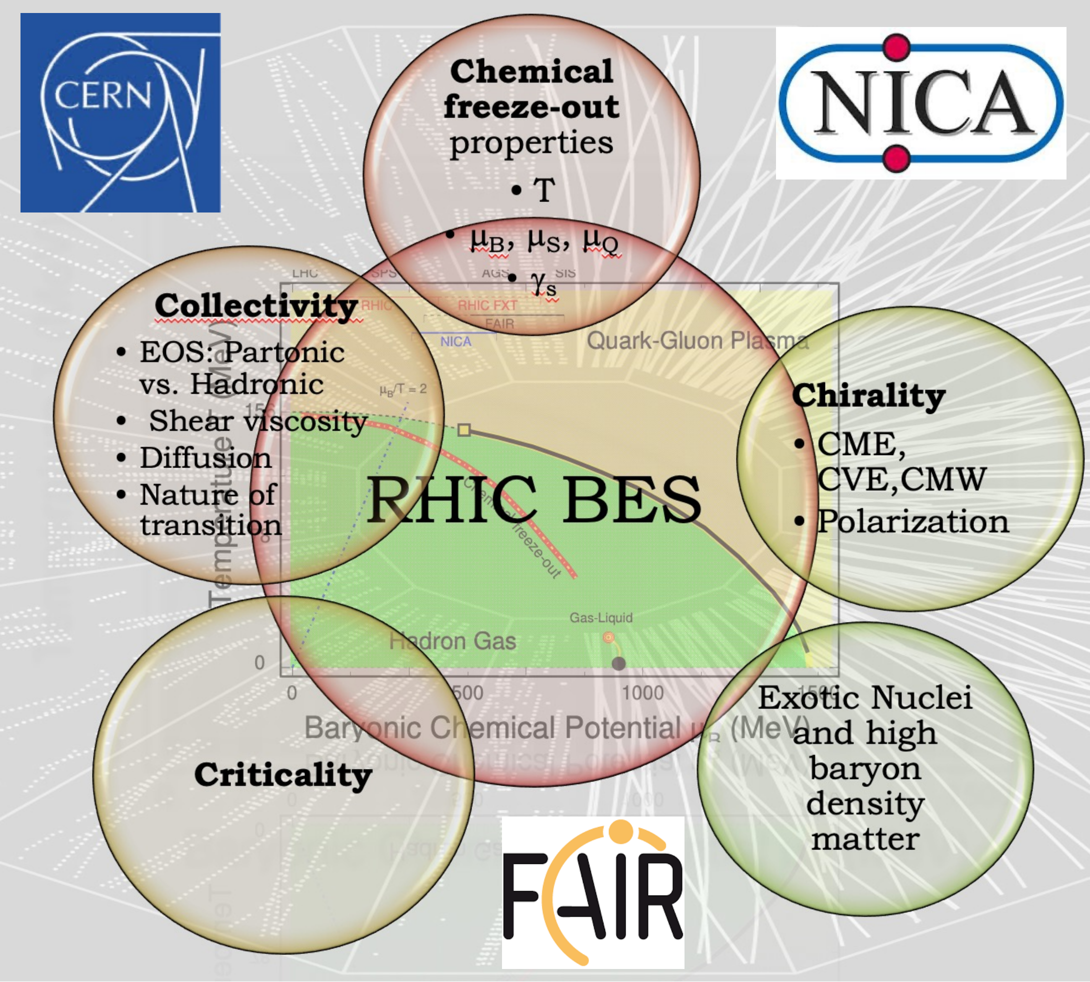

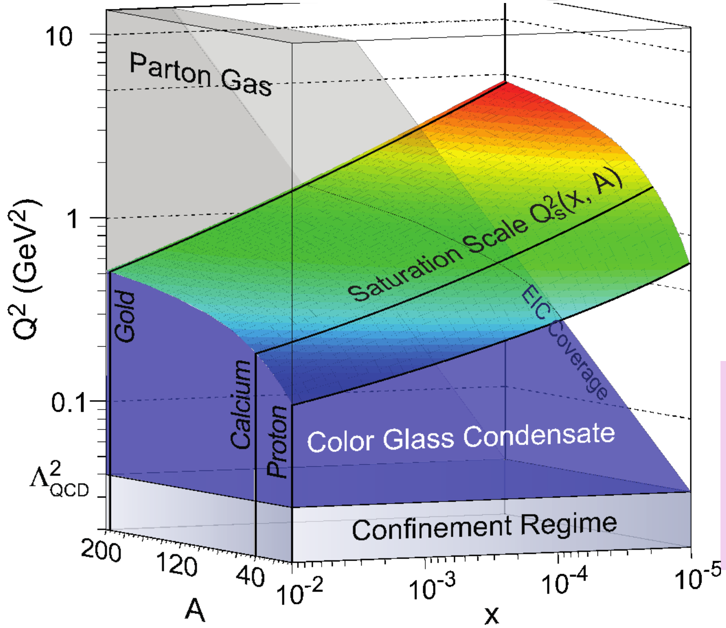

Quest to establish the phase diagrams of cold and hot-dense QCD continues.

Acknowledgements

Frithjof Karsch, Heng-Tong Ding, Jean-Yves Ollitrault, Krishna Rajagopal, Misha Stephanov, Nilmani Mathur, Rajiv Gavai, Sourendu Gupta and Volker Koch.

Thanks for this opportunity

Acknowledgements

Department of Science & Technology, Government of India

Back up

Amplitude of sine-modulation sensitive to hydrodynamic gradients. Data explained by model which incorporates shear induced polarization

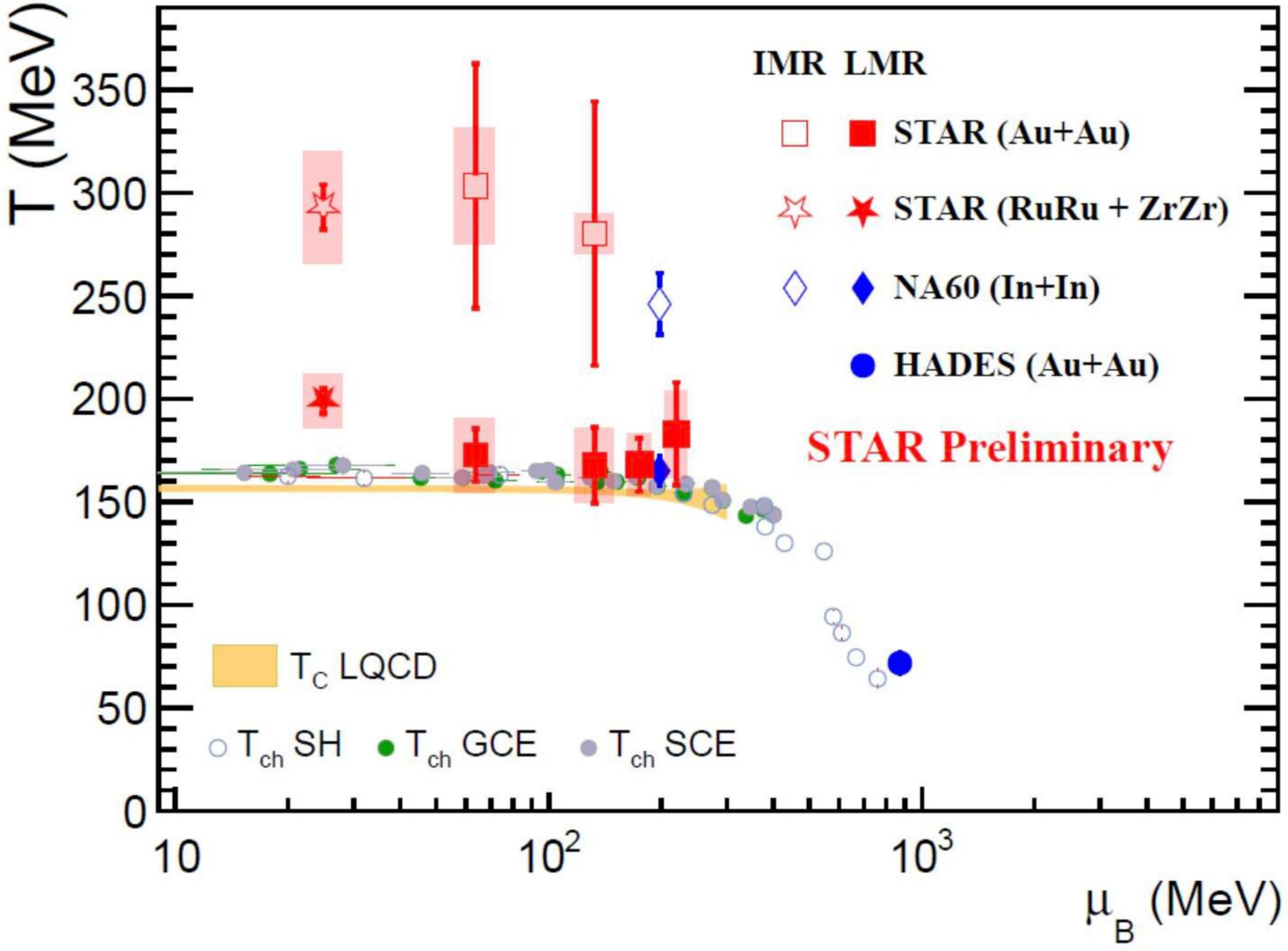

STAR 54.4, 27 GeV: arXiv:2402.01998

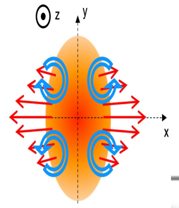

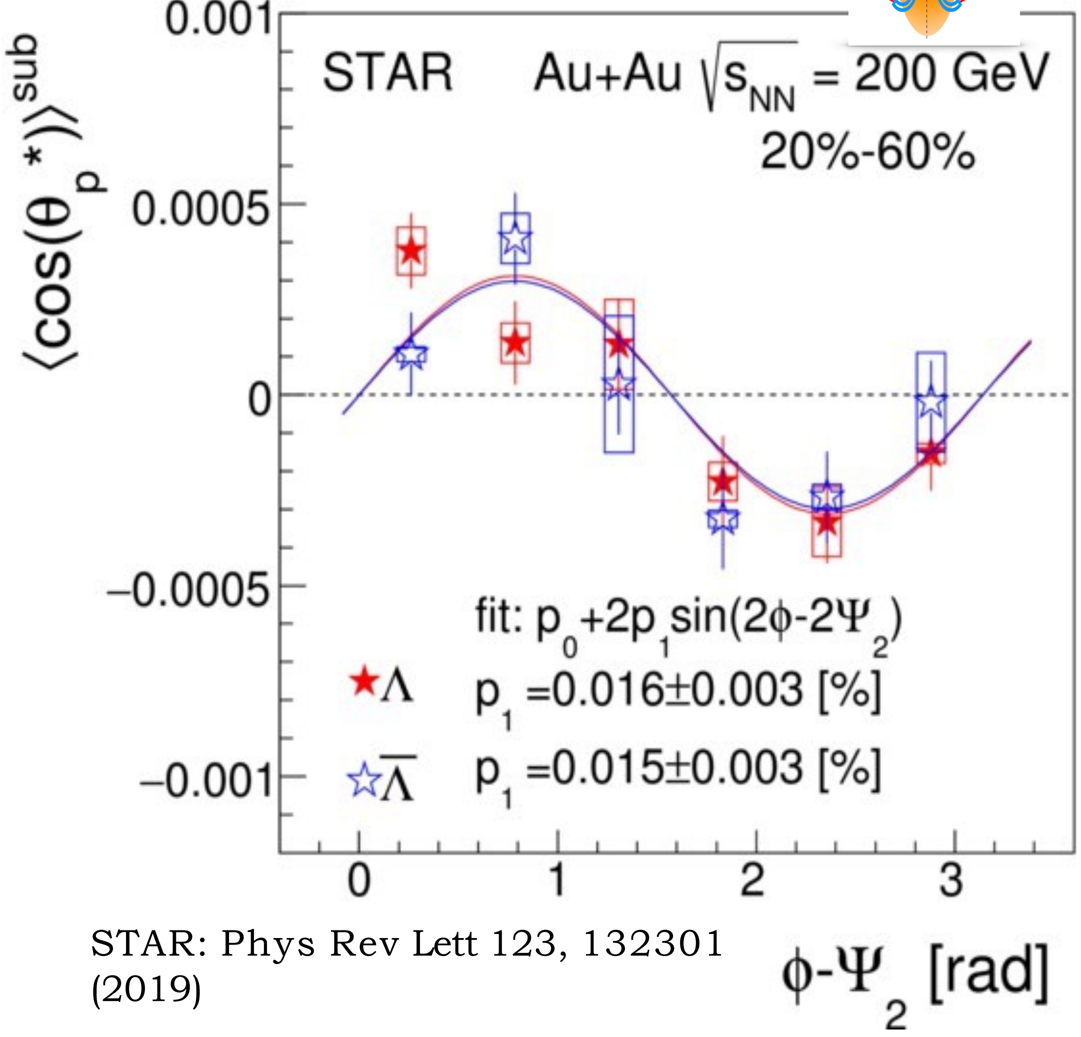

STAR: Phys Rev Lett 123, 132301 (2019)

Fu et., al, Phys Rev Lett 127, 142301 (2021)

Phase structure of QCD

Test of QCD Thermodynamics:
Ordering of net-baryon ratios:
$\frac{C_3}{C_1} > \frac{C_4}{C_2} > \frac{C_5}{C_1} > \frac{C_6}{C_2}$

Theory: HotQCD: PRD101,074502 (2020)

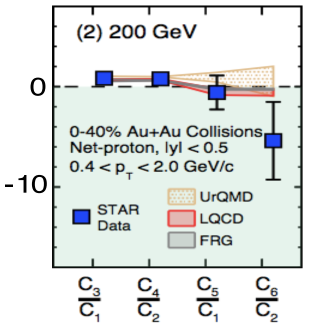

Thermalised QCD matter

Data: STAR: PRC 104, 024902 (2021)
STAR: PRL 127, 262301 (2021)

Search for crossover:
Negative net-baryon $\frac{C_6}{C_2}$

Theory: HotQCD: PRD101,074502 (2020)

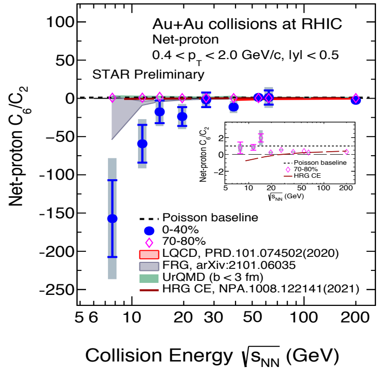

Experimental hint of crossover.

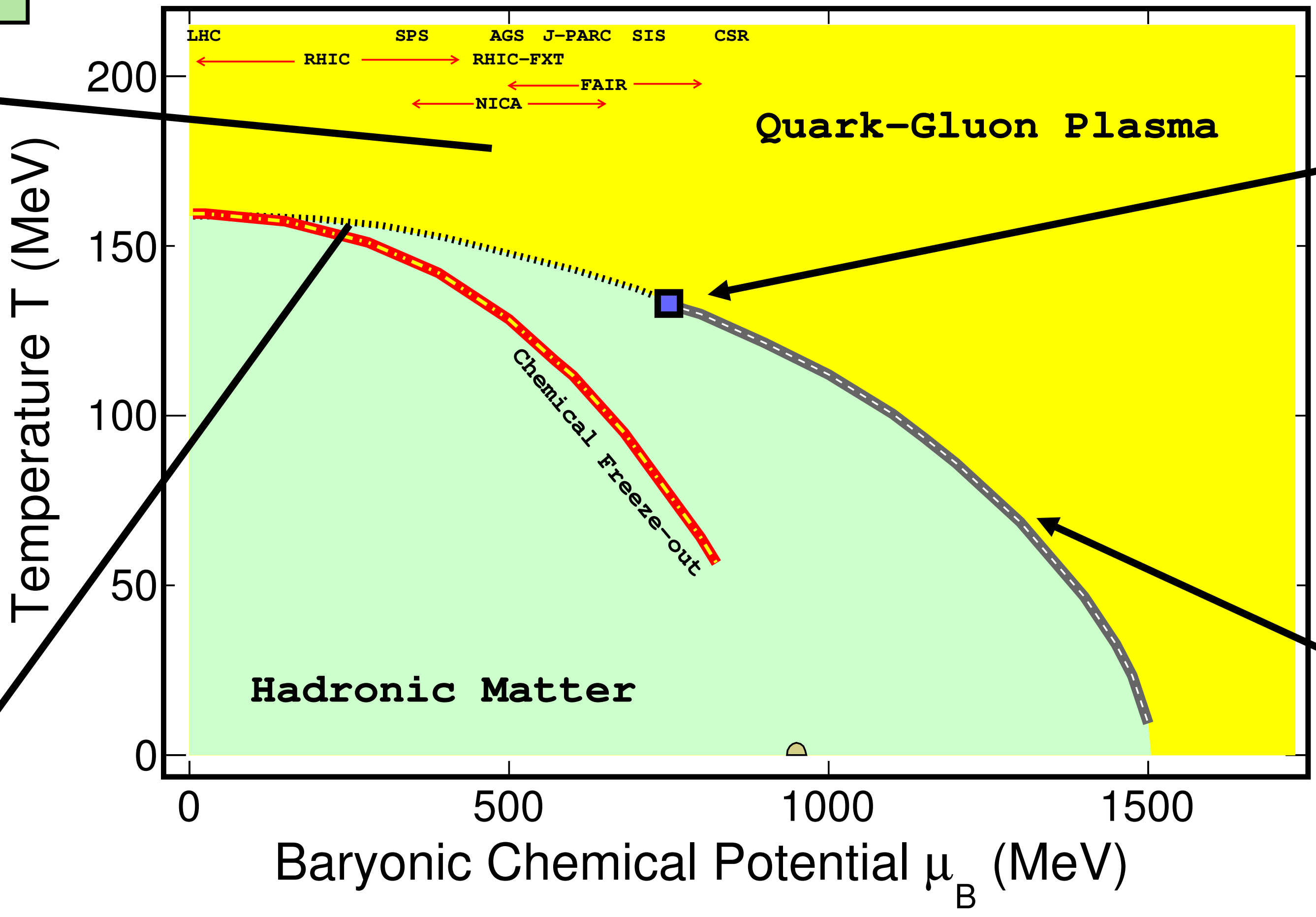

Experimental progress

Search for critical point (CP):
Non-monotonic trend for net-proton Kurtosis C_4/C_2 vs $\sqrt{s_{NN}}$

Theory: M. Stephanov, PRL 107 (2011) 052301

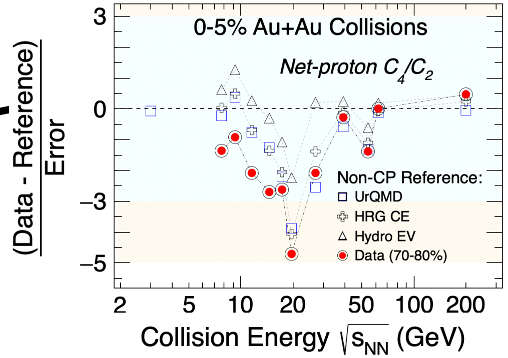

Intriguing experimental result

Data: STAR: PRL 135, 142301 (2025);
PRL 126, 092301 (2021)

Search for 1^{st} order:
Bimodal proton distribution:
Large proton factorial cumulants (κ_5 and κ_6) with alternating sign.

Theory: A. Bzdak and V. Koch, PRC100, 051902(R) (2019)

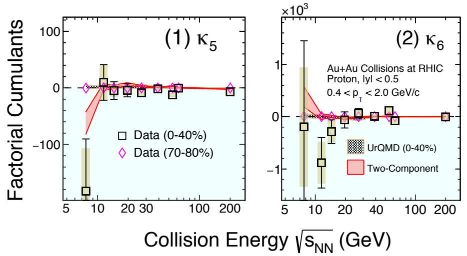

BES-II high statistics data could change the conclusions

Weak signs of first order at very low $\sqrt{s_{NN}}$